HELSINKI UNIVERSITY OF TECHNOLOGY
Faculty of Electronics, Communications and Automation
CZECH TECHNICAL UNIVERSITY IN PRAGUE
Faculty of Electrical Engineering

Uplink MIMO Schemes in Local Area Time Division Duplex System

Master's Thesis

Michal Čierny

Laboratory of Signal Processing and Accoustics
Espoo 2008

HELSINKI UNIVERSITY OF TECHNOLOGY
Faculty of Electronics, Communications and Automation
CZECH TECHNICAL UNIVERSITY IN PRAGUE
Faculty of Electrical Engineering

ABSTRACT OF
MASTER'S THESIS

Author: Michal Čierny

Title of thesis:
Uplink MIMO Schemes in Local Area Time Division Duplex System

Date: August 21 2008 **Pages:** 11 + 74

Professorship: S-88 Signal Processing

Sending supervisor: Prof. Ing. Miloš Klíma CSc.
Receiving supervisor: Professor Risto Wichman

One of 3rd Generation Partnership Projects's release 9 research areas is deployment and improvement of Long Term Evolutions's Evolved Universal Terrestrial Radio Access interface in local area cells, using time division duplex and 100MHz available bandwidth. For uplink part of this system, we revise and study MIMO algorithms considered in release 8's downlink (Cyclic Delay Diversity and Space-Frequency Block Codes open-loop schemes, Singular Value Decomposition and codebook-based closed-loop schemes), look for new alternatives, and simulate impacts of given scenario - reciprocity, correlated MIMO channels, slow fading etc. As a result, we draw conclusions about advantages of having multiple transmit antennas in User Equipment in contrast with higher price and power consumption.

Keywords: Long Term Evolution, MIMO, uplink, local area
Language: English

Contents

List of Figures

List of Tables

Acknowledgements

I would like to thank my supervisor Risto Wichman for giving me the opportunity to work on this project. Through the time of my participation I have probably learned more than through most of my studies before. Although I was only an exchange student, Risto gave me an option to use my time here as good as it gets. I also thank him for his care and feedback throughout these months of work.

At Nokia Research Center, my thanks go especially to Juha Korhonen and Karol Schober, who were always eager to provide answers for the flood of my questions. NRC has been a very motivating environment and seeing the top research in my field of choice was a great experience.

Finally, many thanks to my family, which has always supported me, no matter the distance between us.

Espoo August 21th 2008

Michal Čierny

Abbreviations and Acronyms

3GPP	Third Generation Partnership Project
AoA	Angle of Arrival
AoD	Angle of Departure
ARQ	Automatic Repeat Request
BER	Bit Error Rate
CAZAC	Constant Amplitude Zero Autocorrelation
CDD	Cyclic Delay Diversity
CP	Cyclic Prefix
CQI	Channel Quality Indicator
CRC	Cyclic Redundancy Check
CSI	Channel Status Information
DFT	Discrete Fourier Transform
DFTS-OFDM	DFT-Spread OFDM
DVB-T	Digital Video Broadcasting - Terrestrial
ECR	Effective Code Rate
EDGE	Enhanced Data rates for GSM Evolution
EPC	Evolved Packet Core
FDD	Frequency Division Duplex
FDE	Frequency Domain Equalization
FDMA	Frequency Division Multiple Access
FEC	Forward Error Correction
FFT	Fast Fourier Transform
FN	Frobenius Norm
FSU	Flexible Spectrum Usage
GSM	Global System for Mobile Communications
GP	Guard Period
GPRS	General Packet Radio Service
HARQ	Hybrid ARQ
HLR	Home Location Register
HSDPA	Hifh Speed Downlink Packet Access
HSPA	High Speed Packet Access
HSS	Home Subscriber Server
IDFT	Inverse DFT

IEEE	Institute of Electrical and Electronics Engineers
IMT	International Mobile Telecommunications
IP	Internet Protocol
ITU	International Telecommunication Union
ITU-R	ITU Radiocommunication Sector
LMMSE	Linear MMSE
LOS	Line Of Sight
LTE	Long Term Evolution
LTE-A	LTE-Advanced
MAC	Medium Access Control
MCS	Modulation and Coding Scheme
MIMO	Multiple-Input Multiple-Output
ML	Maximum Likelihood
MMSE	Minimum MSE
MSE	Mean Square Error
MSV	Minimum Singular Value
NLOS	Non-LOS
OFDM	Orthogonal Frequency Division Multiplex
OFDMA	Orthogonal Frequency Division Multiple Access
PAR	Peak to Average Ratio
PDCP	Packet Data Convergence Protocol
PDU	Protocol Data Unit
PHY	Physical Layer
PMI	Precoding Matrix Indicator
PRACH	Physical Random Access Channel
PUCCH	Physical Uplink Control Channel
PUSCH	Physical Uplink Shared Channel
RF	Radio Frequency
RI	Rank Indicator
RLC	Radio Link Control
RNC	Radio Network Controller
RRM	Radio Research Management
SAE	System Architecture Evolution
SC-FDMA	Single-Carrier FDMA
SFBC	Space-Frequency Block Code
SIMO	Single-Input Multiple-Output
SISO	Single-Input Single-Output
SNR	Signal to Noise Ratio
STBC	Space-Time Block Code
SVD	Singular Value Decomposition
TDD	Time Division Duplex
TDL	Tap Delay Line
UE	User Equipment

WAP	Wireless Aplication Protocol
WCDMA	Wideband Code Division Multiple Access
WiMAX	Worldwide Interoperability for Microwave Access
WINNER	Wireless World Initiative New Radio
WLAN	Wireless Local Area Network
ZF	Zero Forcing

Introduction

Wireless communication systems have become an important feature in developed countries. We can not imagine our daily life without at least one radio device with us. Almost everybody has a mobile phone, while more demanding users have more capable smartphones and/or wireless enabled portable computers. The first cellular phone services were only voice-based, but that paradigm is slowly but surely becoming obsolete. Text messages, mobile e-mails, WAP, and most recently general internet connection are supplementing or replacing circuit-switched voice services.

If we focus on cellular networks, the widespread success began with introduction of GSM. While it is not cutting edge anymore, GSM found its way into 212 countries and territories and the infrastructure vendors are still experiencing high demands for it. GSM has been upgraded with GPRS, the cellular deployment of packet-based service, which later evolved into EDGE. The combination of GPRS/EDGE grew very strong. For example in Slovakia, the author's home country, only small part of the territory is not covered by EDGE capable cells. This was a necessary step when it became obvious that 3G deployment is not going to be as fast as expected.

The third genaration, 3G, is the technology of today. Here in Europe it is represented by WCDMA and it is slowly making its way into the market. The growth is not as rapid as we have seen before, partly because it is competing with other systems (FLASH-OFDM in our country) and partly because the demand for mobile internet is lower than the operators would like. WCMDA was later updated with HSPA. Actually, nowadays we would hardly find a 3G cell without at least HSDPA capabilities. This combination already brings the true broadband internet connection to mobile devices.

However, even 3G is going to be surpassed. As the next target, the companies and research community are targeting data rates that have been reachable only by wired connections. If we stick to mobile services, probably the most famous outcomes of such developments are IEEE Mobile WiMAX and 3GPP Long Term Evolution. It seems that performance of the first option is not really satisfactory. As for LTE, it is completely the opposite. It is not an evolution of WCDMA, but as a product of the same standardization consortium, the shift from one to another is expected to be quite smooth. The first demonstrations showed quite promising results and many cellular system operators have already chosen LTE as their future wireless broadband standard.

This thesis is a result of a project between Helsinki University of Technology and Nokia Research Center. With LTE specifications almost finished, the focus is shifting further into the future. As an important part of the evolution, there is a need for deployment in local area environments with a possibility of much higher peak data rates. Such a system would allow sensible installation of base stations in office buildings or shopping malls, or it may be able to

compete with WLAN networks in home or corporate environments.

In LTE, as a result of minimizing the power consumption of a handheld device, only one transmit antenna is allowed for uplink transmission. Thus, no transmit diversity or spatial multiplexing schemes could be deployed. However, with increased pressure also in uplink peak data rates, this has to be revaluated. And this is where our part comes in. We will consider the uplink part of an LTE-based system in wideband and low mobility local area channel and see if MIMO algorithms can provide the means for achieving the necessary performance.

The work is divided into one introductory and three larger chapters. In the beginning, the motivation and goals are further clarified. The second chapter provides basic overview about the most important parts of LTE. We are primarily focused on physical layer, but also some general details will be provided. The third chapter gives an insight into all MIMO schemes that are used in LTE's downlink channel. And finally, the fourth and the most important chapter covers research contribution of our work.

Chapter 1

Motivation and goals

This thesis started as a part of a research project called *Local area TDD*. It was supposed to be focused on deployment and further enhancement of 3GPP's Release 8 standard, or Long Term Evolution (LTE), in local area environment. The plan was to consider bandwidths up to 100MHz in combination with time division duplex. The LTE finalization was running a bit late, therefore no clear requirements were given in the beginning.

The situation changed when ITU-R defined its views on IMT-Advanced system, a next development step of IMT-2000. As a response, 3GPP launched a new Study Item, called LTE-Advanced. The basic target of LTE-A is to fulfill the IMT-A requirements within the ITU-R time schedule and, in addition, to fulfill any other requirements from the operators. The name of our project also changed to *LTE-Advanced*. Its assignment was matched with the new Study Item, but our part remained the same - evaluate multi-antenna transmission schemes in local area TDD uplink.

The main IMT-A requirements are listed here:

- A high degree of commonality of functionality worldwide while retaining the flexibility to support a wide range of services and applications in a cost efficient manner.
- Compatibility of services within IMT and with fixed networks.
- Capability of interworking with other radio access systems.
- High quality mobile services.
- User equipment suitable for worldwide use.
- User-friendly applications, services and equipment.
- Worldwide roaming capability.
- Enhanced peak data rates to support advanced services and applications (100 Mbit/s for high and 1 Gbit/s for low mobility were established as targets for research).

After these were released, 3GPP started to work on LTE-A requirements, resulting in Technical Report [1]. Initial expectations for LTE-A are largely based on IMT-A, however in many cases the targets are set higher. So far, 3GPP has only listed the technical topics to be studied. The actual work is expected to start in the second half of 2008.

The focus of our research team had to be therefore broadened. From a restricted local area deployment, it shifted towards general evolution of LTE with backwards compatibility as one of the essential requirements. From the data rate point of view, 3GPP set the target peak values

at 1Gpps in downlink and 500Mbps in uplink. Although the framework is general, these values are obviously meant for closer range areas with large system bandwidth and low mobility. This is the reason why the goal of our part remained unchanged.

The need for more transmit antennas at the mobile station can be partly justified by simple analysis. For LTE, the uplink peak data rate requirements were set to 50Mbps. The maximum system bandwidth for LTE is 20MHz. In LTE-A, we want to achieve 500Mbps in 100MHz. The data rate level is ten times higher, though we have only five times the amount of bandwidth. This means that the spectral efficiency needs to increased. Target values for peak and average spectral efficiency are also listed in [1], we will not go into details here. The point is, with so many years of research in single-antenna systems behind us, the addition of extra transmit antennas into user equipment seems to be inevitable.

The increase in spectral efficiency can be backed up by MIMO channel capacity formula

$$\mathcal{C} = \log_2 \det \left(\mathbf{I}_{N_r} + \frac{E_s}{N_t N_0} \mathbf{H}\mathbf{H}^H \right), \tag{1.1}$$

where N_t is the number of transmit antennas, N_r is the number of receive antennas, E_s is the symbol energy, N_0 is the power of additive white Gaussian noise, $\mathbf{H}$ is MIMO channel matrix and $\mathbf{I}$ is the identity matrix. The formula presumes zero channel knowledge at the transmitter, therefore the transmission power is distributed evenly across the antennas. By using some algebra, the equation can be rewritten into

$$\mathcal{C} = \sum_{i=1}^{r} \log_2 \left(1 + \frac{E_s}{N_t N_0} \lambda_i \right), \tag{1.2}$$

where r is the rank of the channel and λ_i $(i = 1, 2, \ldots, r)$ are the eigenvalues of $\mathbf{H}\mathbf{H}^H$. This equation represents MIMO channel capacity as the sum of r SISO capacities, each having power gain λ_i and transmit power E_s/N_t. The most important observation is that the capacity grows linearly with adding more antennas. That is the basic motivation of doing so. The equations were cited from [2]. There is also an alternate formula, considering full channel knowledge at the transmitter and thus optimizing also power distribution. However, we will not present it here.

If the increase of data rate is not needed, multiple transmit antennas can still be used to provide additional diversity. The diversity can be picked up by the channel code, thus improving the reception or increasing the cell coverage. Many spatial diversity algorithms have been studied, the relevant ones will be mentioned in Chapter 3. There is one issue - multiplexing and diversity in spatial domain go against each other. We define the multiplexing gain m and diversity gain d by

$$m = \lim_{SNR \to \infty} \frac{\mathcal{R}(SNR)}{\log_2 SNR}, \tag{1.3}$$

$$d = - \lim_{SNR \to \infty} \frac{\log_2(P_e(SNR))}{\log_2 SNR}, \tag{1.4}$$

where $\mathcal{R}(SNR)$ denotes to data rate in terms of bps/Hz as a function of signal-to-noise ratio and $P_e(SNR)$ denotes to probability of error, also as a function of SNR. Then, for each m, the maximum diversity gain that can be achieved is $d_0(m)$. The diversity-multiplexing trade-off is expressed in

$$d_0(m) = (N_t - m)(N_r - m)\ , \quad 0 \leq m \leq \min(N_t, N_r). \tag{1.5}$$

The interpretation is clear - we can deploy maximum possible diversity gain, maximum possible multiplexing gain, or a compromise between those two.

Now, going back to our goal in this work, we do not hope to provide estimates of the actual data rates of the future system. That would be a task for a few people, simulating a lot of effects typical for real environment. But it is not possible here. Our work is the first step in evaluating the improvements provided by multiple transmit antennas. In fact, in order to keep the report in reasonable shape, we limited the number of considered mobile station transmit antennas to two. There is a possibility that an option of including four antennas will be pushed into the standard, but a lot of conclusions can still be made after accepting our restriction.

The actual targets we will attempt to achieve are summarized in the following list:

- We will try to look for the most up to date wireless channel model. We need it to be able to simulate indoor scenarios, high bandwidth, channel evolution via user mobility and antenna correlation. This model will be used to create realistic local area simulation environment.
- We will build a platform capable of simulating link level performance of a wireless system. LTE will be considered as a starting point and our simulator will be built around LTE's uplink specifications. However, several settings (frame structure, etc.) will need to be fitted into wideband local area context.
- All, downlink MIMO algorithms from LTE will be included in the simulation platform. A large amount of research has been done here, therefore introducing these schemes into uplink channel is the most logical way to start exploring uplink multi-antenna capabilities.
- With the simulator ready, we will start modelling different scenarios. At first, properties of the local area channel will be studied. We will look for its strong and weak points and deduce implications for MIMO implementation. Then, all MIMO schemes will be simulated in given channel model. They will be compared with single-antenna case and among themselves. This will be the main focus, leading to important conclusions about MIMO performance in local area uplink. Also, some additional issues will be targeted, most importantly extra options provided by TDD.
- All modeled scenarios will be properly commented, advantages and disadvantages will be evaluated, impacts on existing system will be considered. The gathered material will then be used to draw conclusions about our research topic.

Chapter 2

Long-Term Evolution

Long-Term Evolution is a base stone and starting point of this work. Brief summary of the performance requirements can be found in previous chapter, the original text can be found in [3]. This chapter is dedicated to description of LTE's architecture. We will talk about overall functionality, but keeping in mind the topic of the thesis, the main focus will be put on physical layer procedures. Both uplink and downlink channels will be covered, as downlink, with its thorough MIMO capabilities, can be understood as the reference for improved uplink transmission schemes.

2.1 Architecture overview

To fulfill quite aggresive requirements, LTE, as an evolution of WCDMA/HSPA, had to bring a lot of changes. Though, it is important to say that not only radio access network had to be improved. Parallel to LTE standardization, there is an ongoing work on so called System Architecture Evolution, which is an equivalent attempt to bring a core network of future mobile communication system. SAE, being responsible for higher layers than those in scope of this work, will be briefly described in Section 2.1.2.

A very important thing to start with - the new LTE/SAE network is completely packet based. The worldwide success of Internet is undeniable and calls for IP deployment wherever possible, including wireless communications. It does not mean that traditional circuit-switched services will disappear. The IP network will have to emulate them in order to maintain interoperability.

Packet travel

The IP packets, going from or into the core network, enter our processing chain as *SAE bearers*. Not all types of transmissions follow the same procedure, but usual data packets pass through chain of protocols/layers, which are summarized below. Exceptions, most of them in the form of control information, are out of our scope.

- PDCP - Packet Data Convergence Protocol is responsible for IP packet header compression, ciphering and integrity protection.
- RLC - Radio Link Control segments/concatenates given pre-processed packets, handless retransmission and guarantees delivery of incoming data in correct order.

- MAC - Medium Access Control is a very important entity responsible for hybrid-ARQ retransmissions and uplink and downlink scheduling. The MAC offers services in form of *logical channels*. Because of significant MAC role, a more detailed description is given in Section 2.1.1.
- PHY - Physical Layer, the real starting point of this thesis, handles channel coding, modulation, antenna mapping and other typical physical layer functions. It creates *transport channels* between radio transmitter and receiver. Sections 2.3 and 2.4 describe procedures for both uplink and downlink in quite detailed way.

A few more words about RLC. The segmentation/concatenation part converts *Service Data Units* into *Protocol Data Units* (for transmitter), where the PDU size is determined dynamically. For high data rates, large PDUs with low overhead are preferred, but for lower rates only smaller PDUs ensure acceptable payload. One may also wonder why both RLC and MAC handle retransmission. The reason behind this is that ACK/NACK messages needed by hybrid-ARQ can also be corrupted by noise, which makes another retransmission layer reasonable.

2.1.1 Medium Access Control

The Medium Access Control, sitting beside and above the physical layer, handles logical/transport channel translation, scheduling for both downlink and uplink and controls hybrid-ARQ.

The MAC offers services to RLC in form of logical channels. There are two basic types of them - control (broadcast, paging, dedicated and multicast control channels) and traffic (dedicated and multicast traffic channels). As their names suggest, they provide resources for control information and data, respectively. On the other hand, physical layers provides the system with transport channels. There are also several types of them and they will be described in relevant downlink and uplink sections. One of MAC's responsibilities is multiplexing of different logical channels into these transport channels.

Scheduling

Scheduling for downlink and uplink has the same basic goal - assign resources in time and frequency domain for different users dynamically in a way that provides the best throughput and flexibility. *Scheduler* is a part of MAC that is responsible for this. The way that it works is implementation specific, so each vendor can design his own algorithms for scheduling.

The downlink scheduler works on subframe basis, meaning that it makes its decisions each $1ms$ [1]. Through OFDMA, time and frequency resources are assigned to different users, exploiting the knowledge of channel conditions. The terminal asking for high throuput can be given a lot of bandwidth on frequencies with strong gain, while user with lower requirements is satisfied with simpler MCS (Modulation and Coding Scheme) on weaker frequencies. MCS and antenna mapping (for MIMO algorithms) decisions are also made by the scheduler, but in this case also UE can recommend what is better. UE knows about these things, because while receiving its data it does the estimation of downlink channel. This information, in form of CQI and other indicators, are then fed back to base station.

[1] For frame structure details, please see Section 2.2.1.

Uplink scheduler holds the same function for uplink channel. It gives each user resources in time and frequency domain and makes decision about MCS, which are then reported to each active user. There is one difference from downlink - each user can only be given continuous part of the spectrum. It comes from uplink multiple access scheme, which will be described in Section 2.3.1. Also, channel dependent scheduling is much more complicated for uplink. Estimated the whole bandwidth would require each terminal to sound a part of the spectrum. There is a way to do it, using uplink channel sounding reference signals, but it comes at a cost of bigger overhead.

Hybrid-ARQ

As told before, hybrid-ARQ is the lower part of retransmission control. It is a fast and robust entity, but it is not entirely error free as feedback signalling can also be corrupted.

The abbreviation stands for hybrid - Automatic Repeat reQuest. In wireless communications it is the most widely used error control scheme. Smaller amounts of errors are handled by Forward Error Correction and what cannot be corrected, is retransmitted. The channel code of choice for LTE is turbo code.

LTE uses an extended version of hybrid-ARQ, so called hybrid-ARQ with soft combining. Quite nice short description of this can be found in Section 7.4 of [4]. The idea is that even discarder frames can still carry information which can be exploited when decoding a retransmitted set of bits. LTE uses a soft combining strategy called Incremental Redundancy (IR), where the retransmitted bits do not have to be exactly the same as in the original frame. Instead, they are coded using lower code rate, giving the retransmissions more reliability.

Reporting about correct or incorrect frame reception are done using ACK/NACK messages, which are a part of control signalling. To keep overhead at minimum, each hybrid-ARQ process uses single ACK/NACK bit. To resolve different processes, these bits have to come in specific time instance.

Downlink and uplink hybrid-ARQ work generally in the same way, with one difference. Downlink version is asynchronous, thus the retransmission can occur at any time after the original frame. Explicit hybrid-ARQ process numbers are used to differ parallel processes, and there may be a need for reordering. Uplink hybrid-ARQ uses a synchronous protocol, where retransmissions occur at predefined times. In this case, the process number is easy to derive. Synchronous protocol requires smaller signalling overhead, but it looses part of adaptability to channel conditions. There is a trade-off, but as the base station has only limited information about UE's transmitter, signalling would have to be too big.

2.1.2 System Architecture Evolution

There are two basic types of functions in a cellular wireless system - *radio access network functions* and *core network functions*. Radio access functions are the ones provided by radio interface (i.e. UTRA, E-UTRA), core network functions are necessary mostly from network operator point of view: user charging, quality of service and others. From there, the network is divided into core network and radio access network, Long Term Evolution an System Architecture Evolution in our case, respectively.

In next two lists, functional split between radio access functions and core network functions is showed. The functions of LTE RAN are:

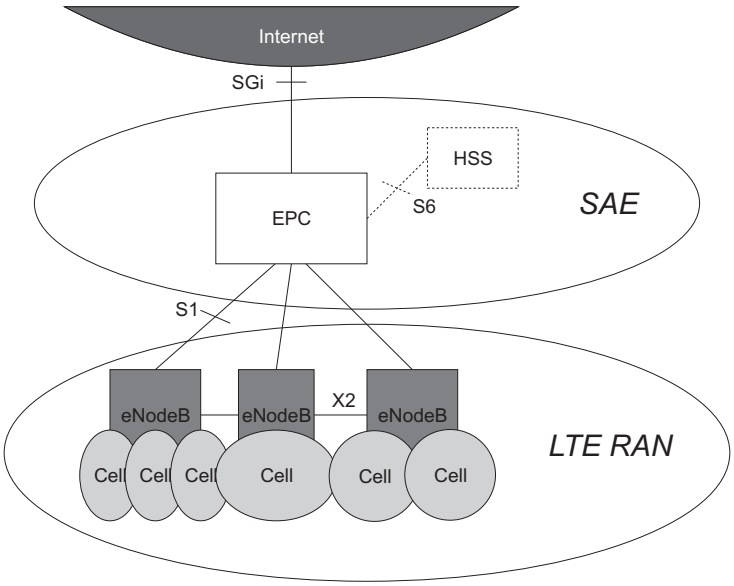

Figure 2.1 *LTE RAN and SAE architecture overview*

- physical layer functions - channel coding, interleaving, modulation etc.
- link layer functions - hybrid-ARQ, header compression, etc.
- security functions - ciphering, integrity protection
- radio resource control functions - handover, resource management, etc.

The functions of core network are:

- charging
- subscriber management
- mobility management (roaming)
- quality-of-service handling
- policy control of user data flows
- interconnection to other networks

From the system architecture point of view, one of important goals of standardization was to minimize number of nodes (base stations, servers etc.). As a result, there is only one type of base station and almost whole core network is centralized into entity. An LTE base station is called eNodeB and the central core network dwells in so called Evolved Packet Core. Figure 2.1 illustrates interconnection between basic blocks of our network. HSS stands for Home Subscriber Server and is a database playing the role of HLR of GSM/WCDMA. It is the only part of core network not sitting in EPC. S1, X2, S6 and SGi are basic interface types connecting LTE RAN and SAE, eNodeBs between each other, EPC and HSS and core network with internet, respectively.

Just like in WCDMA, LTE's eNodeB is in charge over a set of cells. They do not have to share the same antenna site, as well. X2, the interface connecting two eNodeBs, is used only

between neighboring cells. It's main role is to support seamless mobility, but it can also be used for multi-cell RRM.

Comparing the core network with older cellular architectures, the main difference can be found in handling user mobility. The EPC serves as an anchor (fixed node) in the SAE for mobility, meaning that EPC handling a user is never changed during the connection. Also, since EPC takes a role of older network's RNC, it has to be updated on to which eNodeB it shall route the packets of the user. For the interconnection between GSM/WCDMA networks, other types of interfaces are used. SAE also supports roaming, which is done between two EPC nodes: one in the visited network and one in the home network.

2.2 Physical layer commonalities

Flexibility is a key issue in LTE. There are several reasons for this. There is a need for a system deployable on different carrier frequencies and with different bandwidths. And with a given part of spectrum, it should be able to provide throughput from several kilobits to tens of megabits per second, or more. To achieve this, OFDMA and SC-FDMA multiplexing schemes have been chosen, for downlink and uplink respectively. Multiplexing is allowed also in time domain and both FDD and TDD modes are supported.

2.2.1 Frame structure

Basic time unit of LTE, the symbol period, can be expressed as $T_s = 1/(\Delta f \cdot N_{FFT})$. Default subcarrier spacing $\Delta f = 15kHz$, although also $7.5kHz$ is supported for downlink channel. Unless otherwise noted, we will always use the first value. The number of Fourier transform bins N_{FFT} was chosen to be 2048, of which maximum $12 \cdot 110 = 1320$ are used, in order to fit into $20MHz$ bandwidth.

There are two frame structures supported, one for FDD and one for TDD. In both cases, length of one frame is $T_f = 307200 \cdot T_s = 10ms$.

- For FDD, the frame is divided into ten $1ms$ long subframes, of which each consists of two slots. The length of one slot is thus $T_{slot} = 15360 \cdot T_s = 0.5ms$.
- For TDD, one frame consists of two $5ms$ long half-frames, of which each consists of eight $0.5ms$ long slots and three special fields: downlink pilot time slot, guard period, uplink pilot time slot, or shortly DwPTS, GP and UpPTS. Length of these fields depend on actual configuration.

Both downlink and uplink support two lengths of cyclic prefix, normal and extended. With shorter length there are seven OFDM symbols per slot. First of them has 160 symbols long CP, the other have 144 symbols long CPs. In case of extended CP, for uplink it is always 512 symbols long and there are six OFDM symbols per slot. In downlink, for $15kHz$ subcarrier spacing it stays the same and for $7.5kHz$ there are three OFDM symbols per slot with 1024 symbols long CPs.

2.2.2 Resource grid

Resource grid is a map of resource elements in time and frequency domain. A resource element contains a complex symbol on one subcarrier at one time instant. The whole set of resource elements is divided into resource blocks, of which each is (one time slot)x(twelve subcarriers) large. The whole bandwidth is thus made of 110 such resource blocks. To one user the system can assign bandwidth from 6 to 110 of them.

2.3 Uplink

In uplink, user throughput is not the main issue making important decisions. Power efficiency is put right next to it. Having an incredibly fast uplink transmission would be useless if it drains battery power too soon. Though power efficiency is not a main point of this thesis, we should not forget it. Many users prefer long battery time before other features.

This section is dedicated to LTE's uplink transmission, especially physical layer. It is a part for which we want to suggest improvements later, therefore the processing chain is described a bit more in detail than in downlink.

There are three uplink channels defined in LTE: Physical Uplink Shared Channel (PUSCH), Physical Uplink Control Channel (PUCCH) and Physical Random Access Channel (PRACH). PRACH is used when there is no link between user equipment and base station and UE wants to initialize it, PUCCH transmits uplink signalling information if there is no user data to be sent and PUSCH transmits user data multiplexed with uplink signalling. For our work we focus on uplink shared channel. We start by introducing uplink multiplexing scheme, which by introduction into LTE experienced it's premiere.

2.3.1 Single Carrier - Frequency Division Multiple Access

Single Carrier - Frequency Divison Multiple Access, which is based on a transmission scheme called DFTS-OFDM, was chosen for LTE's uplink channels for these reasons:

- Low PAR. 'Single carrier' property ensures that variations in the instantaneous power of transmitted signal are kept low.
- Straightforward application of equalization in frequency domain. FDE requires less computational power in larger bandwidths and with time/frequency domain transformations are already present, its deployment fits nicely.
- Access to frequency domain in order to apply FDMA with flexible bandwidth assignment.

Basic DFTS-OFDM structure can be found in the transmitter part of Figure 2.2. There is an inverse DFT, typical for OFDM, preceded by DFT. The number of samples in DFT M is always smaller than N, size of IDFT. A signal created in this way keeps the 'single carrier' property. It's bandwidth and place in spectrum is determined by ratio $\frac{M}{N}$ and positioning of M transformed symbols into M of N IDFT input bins. This fact is used in user multiplexing, where unused IDFT bins can be assigned to other users. Unlike in downlink, each user has to use continous part of the spectrum in order to maintain the 'single carrier' property. After the N sized IDFT, in the same manner as in OFDM, follows an addition of cyclic prefix.

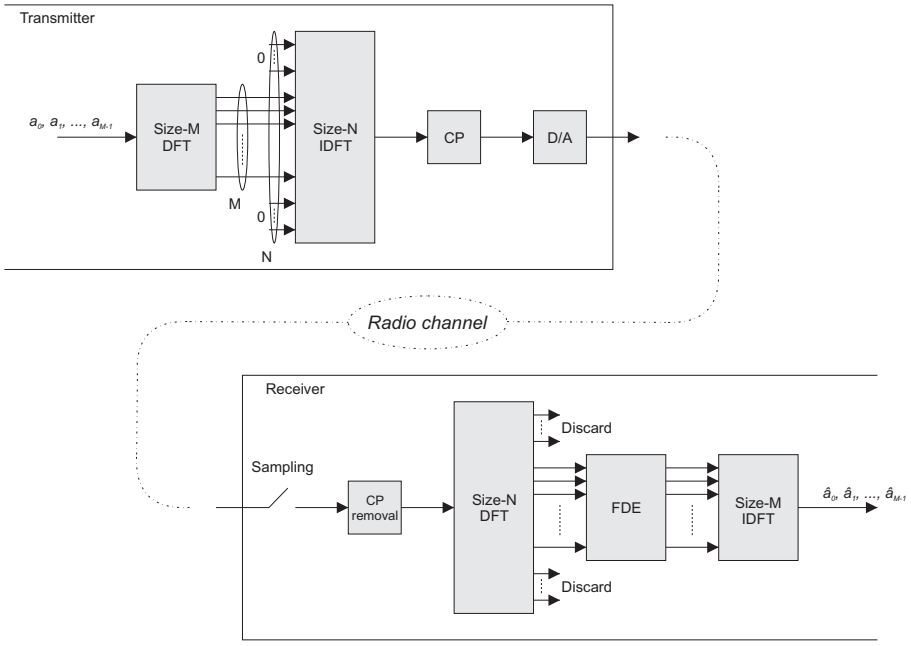

Figure 2.2 *Basic SC-FDMA transmitter and receiver structure*

On the other part of Figure 2.2 there is a basic receiver structure. It performs operations inverse to those at the transmitter and includes one additional block. FDE stands for Frequency Domain Equalization and it is one of the strong advantages in OFDM and DFTS-OFDM transmission schemes. The idea was published in [5]. While in time domain the channel is represented by it's impulse response, in frequency domain we use spectrum. Logically, spectrum of the channel can be obtained by applying DFT. The advantage here is that instead of convolution in time domain, we can use multiplication in frequency domain (symbol on bin i is multiplied by equalizing coefficient w_i). For higher bandwidths, this represents important reduction of computational complexity.

2.3.2 Processing chain

In UL-SCH multiplexed data and control information have to go through several processing steps before being transmitted. An overview of this chain can be seen in Figure 2.3. The DFTS-OFDM is not in the figure, as it was described before.

CRC insertion

As a first step, Cyclic Redundancy Check tail bits are added at the end of a block. In the receiver, the integrity is checked and if error is found, hybrid-ARQ protocol is asked for retransmission.

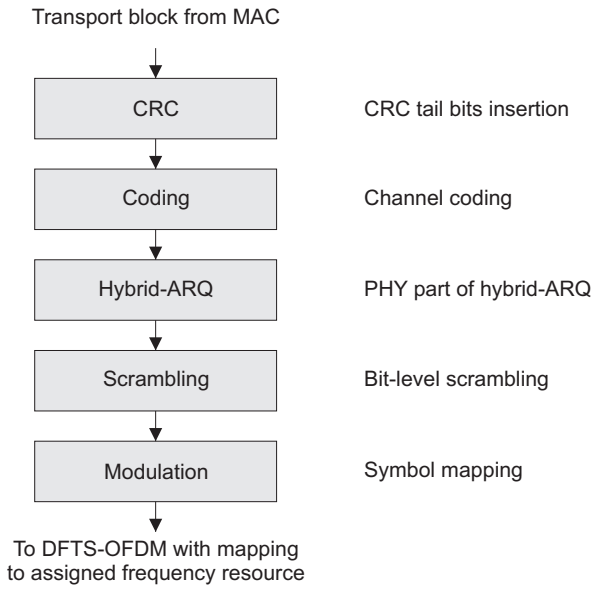

Figure 2.3 *LTE uplink transport channel processing*

Channel coding

LTE uses Turbo coding as a forward error protection measure. The encoder consists of two 1/2 rate, eight state convolutional sub-encoders and a Quadrature Permutation Polynomial interleaver, with a overall code rate $R = 1/3$. Decoding is implementation specific, meaning that each vendor can choose the type of decoder on his own. Detailed specifications about channel coding are in [6].

Physical-layer hybrid-ARQ functionality

Physical layer part of hybrid-ARQ protocol has to align number of bits to be transmitted with number of available bits in assigned resources. If there is not enough resources, hybrid-ARQ takes a subset of transport channel bits, leading to effective code rate $R_{eff} > 1/3$. On the other hand, if number of code bits is smaller than available resources, the protocol repeats all or part of the bits, implying $R_{eff} < 1/3$. If retransmission is necessary, because of Incremental Redundancy allowed, hybrid-ARQ can generally select a different set of coded bits.

Bit-level scrambling

Scrambling consists of multiplication of code bits with user specific scrambling sequence. Main purpose of scrambling is interference randomization, so that the receiver can after de-scrambling fully utilize processing gain of used channel code. The sequences itself are length-31 Gold codes defined in [7].

Data modulation

Data modulation maps given scrambled bits into complex symbols. In UL-SCH, LTE supports QPSK, 16QAM and 64QAM constellations. For other channels, restrictions can apply. Exact bit to symbol mapping can also be found in [7].

2.3.3 Reference signals

In order to perform coherent signal demodulation, receiver needs to be provided with sufficiently precise channel estimate. The most efficient way to do that is using one of many data-aided algorithms, where the estimator knows both tranmitted and received symbols and can thus try to compute what happened inbetween. The signals used for this are pre-defined and are called *reference signals*.

There are two basic types of reference signals in LTE's uplink transmission. *Demodulation reference signals* and *sounding reference signals*. The former are used in a way described a few lines above and are transmitted in the middle of each time slot, placed on the same set of subcarriers as user data. The latter are used for uplink scheduling and follow a bit more difficult pattern, with details in [7] and [8].

Good reference sequences should preferably have several properties:

- Little or none amplitude variations in order to fit into uplink low PAR philosophy.
- Single peak auto-correlation function in time domain to allow for accurate channel estimation.
- Possibility of creating multiple sequences with low cross-correlation.

Sequences possesing ideal versions of the first two properties are known in research community as *constant amplitude zero autocorrelation* (CAZAC) sequences. To further clarify the third property - we do not need to distinguish different users in single cell. They sit on different subcarriers and can therefore use the same reference sequence. However, there may exist a strong interference between two cells, the closer they are the worse. In order to avoid complicated cell planning, larger number of orthogonal sequences is desired.

It may seem that describing reference signal details is not relevant for this work, but it is not the case. In case of multiple transmitt antennas, we need to estimate channels from all of them (in next chapter we will talk about channel matrix, which encapsulates channels between all transmitt and receive antennas). If reference signals for different antennas are transmitted on the same time-frequency resources, the low cross-correlation property comes in handy again.

Reference signal generation

To get as close to given requirements as possible, 3GPP devided reference signal definition into two parts. For bandwidths smaller than three resource blocks the sequence is defined manually in [7] and for larger ones they are based on *Zadoff-Chu* sequences [9]. Thorough definition can be found in the specification, here we will describe only their most important properties.

Generally, a Zadoff-Chu sequence of odd length M_{CZ} is defined in frequency domain by

$$X_{ZC}^{(u)}(k) = e^{-j\pi u \frac{k\cdot(k+1)}{M_{ZC}}}, \tag{2.1}$$

where u is a index in a set of sequences with the same length. They belong to above mentioned CAZAC sequences, meaning that their autocorrelation has only one non-zero value. For given sequence length M_{ZC}, the number of possible sequences (values of u) is equal to the number of integers that are relatively prime to M_{ZC}. From that, the number of possible sequences in a set is maximized if M_{ZC} is a prime number, therefore in LTE the closest prime number smaller than used number of subcarriers is taken. To fit into given resource sequence is then cyclically extended. The definition used for the system is a bit more complicated - for bandwidths smaller than 6 resource blocks there are 30 allowed sequences from the set, for larger ones there are 60.

When planing a multi-cell deployment, the desired minimum cross-corellation properties can be achieved in two ways - taking two different Zadoff-Chu sequences from the same set (same M_{ZC}, but different u), or relying on zero-autocorrelation property of single sequence, achieved by introducing a cyclic shift. If the cyclic shift is longer than channel delay spread, sequences will be orthogonal. There is one more interesting property - the sequence is CAZAC, only if DFT of the sequence is CAZAC. In our case, DFT of a Zadoff-Chu sequence is again a Zadoff-Chu sequence.

2.4 Downlink

When boasting about system performance, people usually compare the speed they can achieve when downloading data. This leads to putting more pressure on downlink channel. In our case, goal of the work is to analyze uplink improvements, using multiple transmitt antennas. However, a vast amount of research work has been done in downlink MIMO algorithms. That is why we dedicate this section to it and use it as reference starting point.

The multiplexing scheme of choice in downlink is OFDMA. OFDM is a famous modulation scheme already used in many systems (WiMAX, WLAN, DVB-T), OFDMA adds putting different users on different subcarriers. In LTE, it is done in the manner as was described in Section 2.2.2, each user can be awarded a bandwidth 6 to 110 resource blocks wide, in discrete steps listed in [10]. The resource blocks do not have to be neighbouring each other here.

For several years now, OFDM has been a favourite transmission scheme. Some of the reasons behind this are listed here:

- Relatively long OFDM symbols with cyclic prefix provide high degree of robustness against channel frequency selectivity. For bandwidths above $5MHz$, equalization in frequency domain makes much more sense that classical TDL equalizers.
- Flexible bandwidth allocations are easily supported by OFDM.
- Subband-based adaptive modulation and coding scheme. Possibility of flexible MCS choice provides robustness against frequency selectivity.
- Broadcast and multicast transmission with several base stations sending the same data is straightforward with OFDM.

Comparing the uplink and downlink scheme, there are a few important differences, which need to be kept in mind. First of all, the downlink spectrum in one cell is transmitted from single base station, whereas uplink spectrum is build from all connected user equipments. This is typical for all cellular systems and there are important consequences. Two examples are given here:

- The base station has knowledge about all the active users. The benefit can be for example seen in possibility of spatial beamforming or rejecting interference from unnecessary users.

- The base station can sound the whole spectrum with reference symbols, which can be received and used by all users. On the other hand, the users themselves can send pilot symbols in band only a bit wider than their assigned bandwidth. An ideal case would be when both users and base station have good knowledge of whole bandwidth. As an example, we give two consequences:
  - Computation of best downlink MCS, PMI and RI is done in user equipment, consuming processing time and raising price of the cellular phone
  - Uplink schedulink, which is done in base station, is based on weaker uplink reference symbols.

Other already mentioned difference, crucial for this work, is a presence of multiple transmit antennas in base station. They are not mandatory, but can increase performance (throughput, coverage) significantly. We will describe them in Section 2.4.2. There are six types of channels defined in LTE downlink. For their list and detailed description the reader is reffered to [7]. From now on, we are interested only in Physical Downlink Shared Channel (PDSCH).

2.4.1 PDSCH processing chain

User data in form of transport blocks coming from MAC layer are transmitted from base station to user equipment through Physical Downlink Shared Channel. Physical layer is responsible for preparing transport blocks into digital samples which can be sent into D/A converter and further down the transmitter RF chain. Overall structure of PDSCH processing procedure can be seen in Figure 2.4. We can see two identical chains there, but the second one is used only in case of spatial multiplexing, as we will talk about later. We have seen almost all of the processing blocks already in uplink, nevertheless, a short description is given in following list.

- *CRC insertion:* Similar to the uplink, CRC tail bits are appended for residual error detection.
- *Channel coding:* Forward protective coding, same set of Turbo codes as in uplink.
- *PHY of hybrid-ARQ:* Fitting number of input bits into number of bits available for transmission (by adjusting effective code rate). Retransmission control with Incremental Redundancy.
- *Scrambling:* Multiplying bit sequence with randomization code, which leads to interference reduction after de-scrambling. Same as in uplink.
- *Modulation:* Also same as uplink transmission. QPSK, 16QAM or 64QAM can be used.
- *Antenna mapping:* Mapping single or multiple data layers into single or multiple transmitt antennas. More details in Section 2.4.2.
- *Resource mapping:* Mapping into resource blocks assigned by MAC scheduler, for each antenna.

2.4.2 MIMO options

Multi-antenna techniques are the main reason beyond downlink's superior peak data rates, when comparing with uplink. That is achieved by spatial multiplexing, where two or more layers of

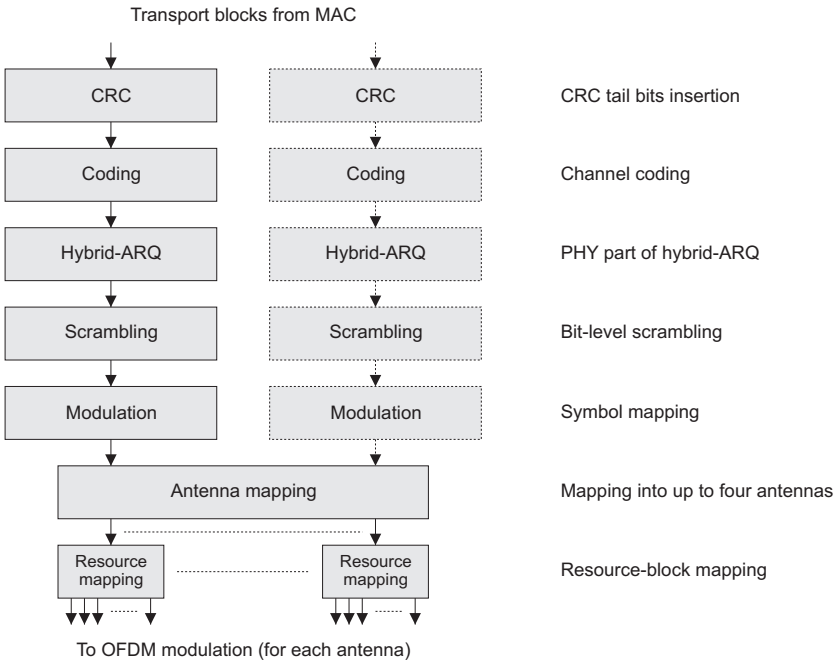

Figure 2.4 *LTE downlink transport channel processing*

data are transmitted, mostly in good SNR conditions. However, also in weaker areas, single-layer reception can be significantly improved by means of spatial diversity or beam-forming. The former of these two takes advantage of statistical properties of wireless channel and the latter tries to adjust phases of transmitted signals so that they add constructively on the receiver side. In this small section we will list all techniques suported by LTE, while thoretical and performance details will be provided in Chapter 3.

To define different MIMO techniques in a convenient way, LTE divides antenna mapping into two operations: layer mapping and precoding. As we can see in Figure 2.5, up to two turbo-codewords, four layers and four antennas are supported. Two codewords mean that there are two parallel processing chains, as described in Section 2.4.1. They are used in case of spatial multiplexing, and if more than two layers are required, one or both of the chains run at double speed. Layer mapping maps codewords into layers and antenna mapping spreads these layers across one, two or four transmitt antennas, by means of matrix multiplication.

Open-loop transmit diversity

LTE supports Space-Frequency Block Coding for two and four antennas as an open-loop MIMO mode. There is a single codeword de-multiplexed into two or four layers, on which the precoder applies space-frequency code matrix in the form defined in [7]. As SFBC is an open-loop method, it does not require any dedicated feedback. The receiver though has to know if it is used, otherwise it would not be able to decode the signal. More about SFBC in Section 3.2.

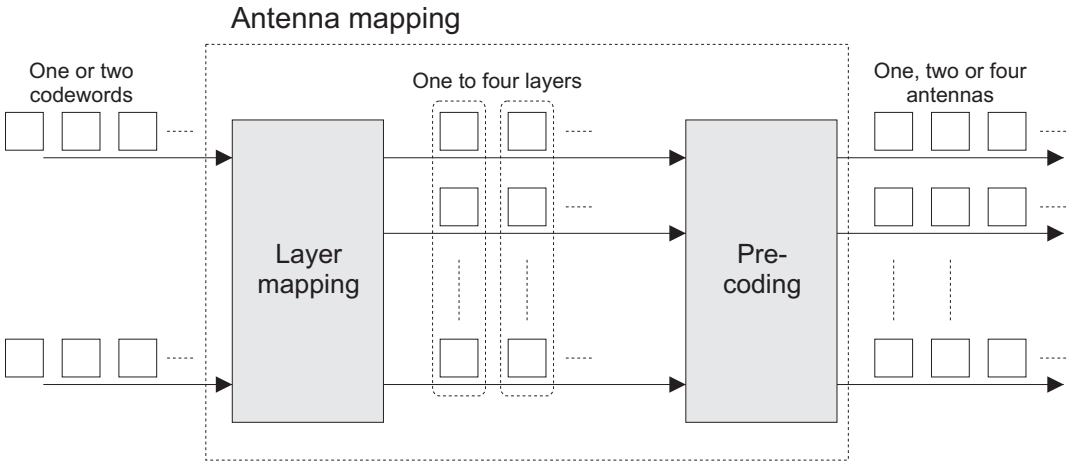

Figure 2.5 *Antenna mapping in LTE downlink*

Open-loop spatial multiplexing

In LTE, the mode that supports open-loop spatial multiplexing is called *large delay Cyclic Delay Diversity*. The mode is described in [8] with further details in [7]. It can be applied on two to four layers and two or four transmit antennas. The precoding matrix is selected from codebook used for closed-loop schemes. In case of two antennas the matrix is fixed and in case of four antennas it is periodicaly changing between four matrices from the set. This scheme will be simulated and described in more details in Section 3.3.

Codebook-based beam-forming and spatial multiplexing

Closed-loop code-book part of LTE's MIMO capabilities seems to be the most promising one. The idea is that UE measures properties of the channel and sends the information back in form of recommended *Rank Indicator* (RI) and *Precoding Matrix Index* (PMI). RI is a recomended number of layers, PMI is a index of recommended precoding matrix in codebook. If only one layer is transmitted, we are talking about beam-forming, more layers mean spatial multiplexing.

The closed-loop mode can work either in wideband or in frequency selective mode. Wideband mode uses a single precoding matrix for all subcarriers assigned to a user while frequency selective mode allows granularity. Size of a subband with it's own CQI, PMI and RI is defined in [8]. It differs for different system bandwidths. Performance improvement by using subbband mode can be quite high, especially in frequency selective channels.

As an addition, closed-loop scheme could be used in combination with *small delay Cyclic Delay Diversity*. It is a transmit diversity scheme applicable for OFDM transmissions, where the spatial diversity is transformed into frequency diversity. It is done by introducing different cyclic shifts for different antennas. Although this possibility was removed in the last version of specification, we present details in Section 3.1.

Chapter 3

LTE's multi-antenna transmission

In Section 2.4.2 we briefly introduced multi-antenna capabilities of Long Term Evolution's downlink channel. This chapter goes deeper into details. It defines all schemes that are in 3GPP specification, and mentions some of those that did not make it into it. We will define all options by mathematical notation and, if possible, also by block diagrams.

In order to see the benefits of multiple transmit antennas immediately, after each definition we will present simulation results of idealized systems. As performance measures we will use either bit error rate (BER) or throughput curves, depending on number of transmitted layers. In case of BER, channel coding will be included only when necessary. Throughput simulations use CRC tail bits and 3GPP Turbo coding, where the throughput itself is calculated from OFDM symbol error rate.

We will begin the chapter by defining signal model, which is used in every scheme's description. After that, a short information about used receiver algorithms concludes the introduction.

Signal model

Time domain baseband received signal in basic single-path MIMO channel with N_t transmit and N_r receive antennas is given by

$$\mathbf{y} = \mathbf{H}\mathbf{x} + \mathbf{n}, \tag{3.1}$$

where $\mathbf{y}$ is a $N_r \times 1$ vector of received symbols, $\mathbf{H}$ is a $N_r \times N_t$ channel matrix, $\mathbf{x}$ is a $N_t \times 1$ vector of transmitted symbols and $\mathbf{n}$ is a $N_r \times 1$ additive noise vector. If the channel is multi-path, each element of channel matrix $\mathbf{H}$ is a impulse response vector. In that case, received signal can be expressed as

$$y_i(t) = \sum_{j=1}^{N_t} h_{i,j}(t) \star x_j(t) + n_i(t) \ , \quad i = 1, 2, \ldots, N_r. \tag{3.2}$$

In this case y, h, x, n are elements of $\mathbf{y}$, $\mathbf{H}$, $\mathbf{x}$, $\mathbf{n}$, t is a discrete time index and $\star$ is a convolution operator. If we now shift into frequency domain with subcarrier index k, our model will be

$$\mathbf{y}(k) = \mathbf{H}(k)\mathbf{x}(k) + \mathbf{n}(k). \tag{3.3}$$

This is the model we will use most often. Even if frequency index k is omitted, we will always refer to frequency domain model, not (3.1). For convenience, we will also often omit noise term $\mathbf{n}$

A concept of equivalent channel will be used quite often in this section. We show its meaning on a beam-forming example, where $\mathbf{W}$ is a $N_t \times 1$ vector which changes phases of transmit antennas in order for spatial signals to combine constructively at the receiver:

$$\mathbf{y} = \underbrace{\mathbf{HW}}_{\mathbf{H}_{eq}}\mathbf{x} + \mathbf{n}, \tag{3.4}$$

where $\mathbf{H}_{eq}$ is the equivalent channel matrix.

MIMO receivers

Plenty of literature can be found on different types of MIMO receivers. From basic *zero forcing* (ZF), *minimum mean square error* (MMSE), *maximum likelihood* (ML) to more complicated structures like *successive interference canceler* or joined detection/decoding *Turbo equalizer*. However, receiver structure is not in focus of this work. Therefore, we will use simple and widespread *linear minimum mean square error* (LMMSE) equalizer.

Advantages of LMMSE equalizer are very low computational requirements, and no complexity increase when used with higher order modulations. The equalized symbols $\mathbf{r}$ are given by

$$\mathbf{r} = \mathbf{G}_{LMMSE}\mathbf{y}, \tag{3.5}$$

where weighting matrix $\mathbf{G}_{LMMSE}$ is (with σ^2 being noise power)

$$\mathbf{G}_{LMMSE} = \left(\mathbf{H}_{eq}^H\mathbf{H}_{eq} + \sigma^2\mathbf{I}\right)^{-1}\mathbf{H}_{eq}^H. \tag{3.6}$$

3.1 Cyclic delay diversity

Cyclic delay diversity (CDD) is a logical extension of delay diversity for OFDM based systems. Delay diversity is a simple idea originating from systems making an advantage of multi-path radio channel, resulting in frequency diversity. In an frequency-flat environment, multiple transmit antennas can be used to introduce artificial frequency diversity by transmitting the same signal with different delays from the extra antennas.

In OFDM, the channel code can strongly benefit from increased frequency diversity. However, if additional delay leads to an echo exceeding cyclic prefix, it may bring up inter-symbol interference. CDD overcomes this problem by doing different cyclic shifts on multiple transmit antennas. In addition to its simplicity, CDD does not cause rate loss nor require any receiver changes.

In the next sections we will define CDD in more detail, using figures and formulas. We will also show how it was used in LTE, before the removal. And at the end we will present basic performance comparisons with single antenna transmission. For further reading, interested reader is referred to original paper [11].

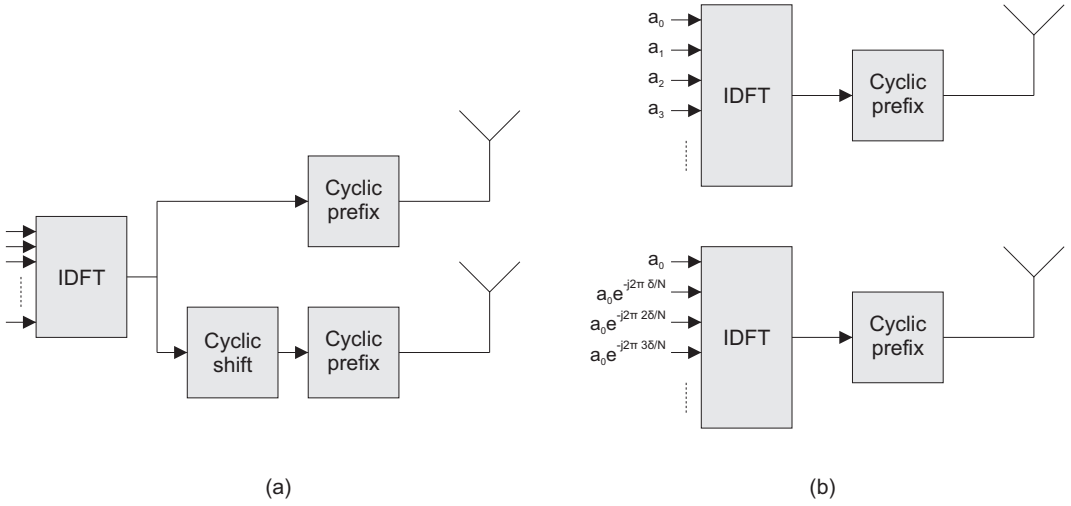

Figure 3.1 *Cyclic delay diversity in time and frequency domain*

3.1.1 CDD definition

The basic idea behind CDD is shown in Figure 3.1. On the (a) side there is a time domain implementation. It is already drawn for OFDM, but without IDFT and cyclic prefix it is valid for general transmission scheme. Keeping in mind DFT rule for time shifted signal, (b) part shows a frequency domain version, which is more convenient for OFDM.

Following the frequency domain implementation, we can define transmitted signal using CDD according to

$$s\left((n-\delta) \mod N\right) = \frac{1}{\sqrt{N}} \sum_{k=0}^{N-1} e^{-j\frac{2\pi}{N}k\delta} a_k \cdot e^{j\frac{2\pi}{N}kn}, \tag{3.7}$$

where n stands for time domain index, k for frequency domain index, N is an IDFT size and δ is the length of applied cyclic shift for given antenna. On the RHS, first exponential is for cyclic shifting, the second belongs to IDFT. The following definition was valid before version 8.3.0 of [7], where small delay CDD was removed.

$$\begin{bmatrix} y^{(0)}(k) \\ \vdots \\ y^{(N_t-1)}(k) \end{bmatrix} = \mathbf{D}(k)\mathbf{W}(k) \begin{bmatrix} x^{(0)}(k) \\ \vdots \\ x^{(\nu-1)}(k) \end{bmatrix} \tag{3.8}$$

It is a general precoding definition for ν layers and N_t transmit antennas. $\mathbf{D}(k)$ is a CDD matrix and $\mathbf{W}(k)$ is a $N_t \times \nu$ codeword used for codebook-based closed-loop transmission, x are symbols to be transmitted and y are symbols after precoding. For two antennas and simple transmit diversity, which is relevant for this section, there would be a single layer and the matrices would look like

$$\mathbf{D}(k) = \begin{bmatrix} 1 & 0 \\ 0 & e^{-j2\pi k\frac{2}{\eta}} \end{bmatrix} \quad , \quad \mathbf{W}(k) = \frac{1}{\sqrt{2}} \begin{bmatrix} 1 \\ 1 \end{bmatrix},$$

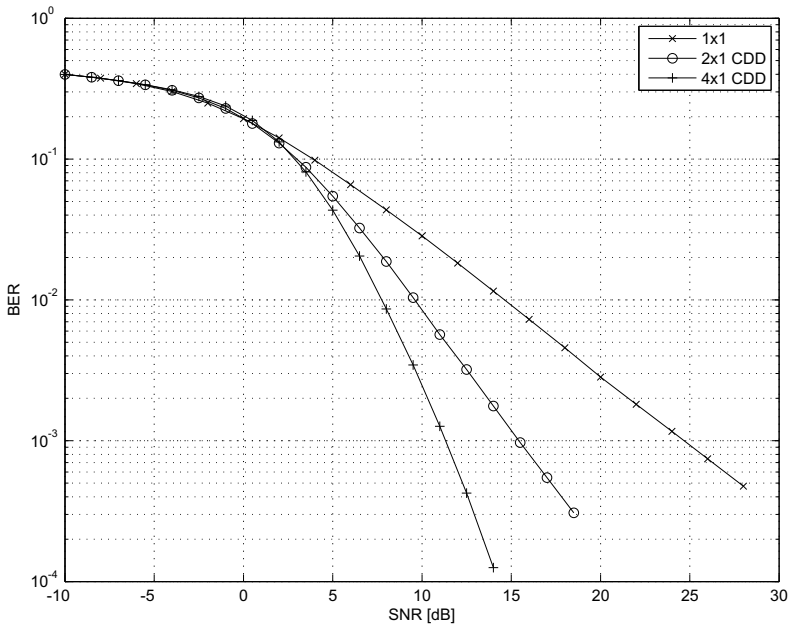

Figure 3.2 *Bit error rate curves for CDD*

where η is the smallest number from {128,256,512,1024,2048}, which is larger than number of assigned subcarriers. In our signal model, CDD matrix is embedded in equivalent channel matrix (3.9), which means that receiver does not need to be changed. However, it has to know the equivalent channel, which can be achieved for example by applying CDD matrix also on reference symbols.

$$\mathbf{H}_{eq}(k) = \mathbf{H}(k) \cdot \mathbf{D}(k) \tag{3.9}$$

3.1.2 CDD performance simulation

For very basic performance plots, a lightweight simulation script was created. Unlike other MIMO schemes in this chapter, channel coding must be present in order for CDD to work. Simulation parameters are summarized in following list.

- OFDM transmission with 512 FFT bins, 300 are used.
- Block fading with one channel realization per OFDM symbol.
- QPSK modulation.
- 3GPP Turbo coding, 1/2 effective code rate, single Turbo codeword per OFDM symbol, no interleaving.
- Frequency flat Rayleigh channel, no spatial correlation.
- FDE LMMSE receiver with full channel knowledge.

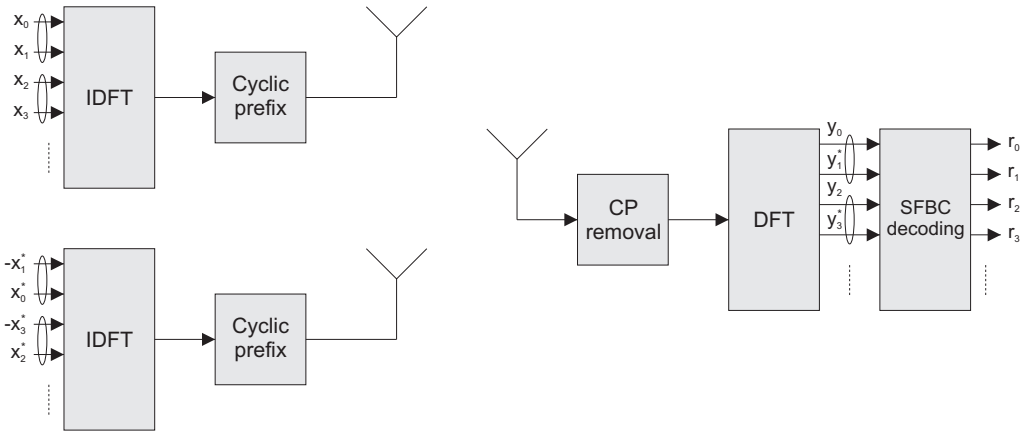

Figure 3.3 *Space-frequency code transmitter and receiver*

Results are shown in Figure 3.2. X-axis values SNR stand for signal to noise power ratio. Unit power per used FFT bin is transmitted. We compared single antenna transmission with CDD scheme for two and four antennas. Until approximately 1dB SNR, SISO system performs a very small bit better. The reason is that with such an error rate the channel code breaks down and even worsens the result. In higher SNRs, CDD gain over SISO system is high, while improvement from two to four transmit antennas is smaller.

3.2 Space-frequency block codes

LTE's basic multi-antenna transmission scheme, which is used if the principal closed-loop scheme fails, is space-frequency block coding. In SFBC, modulation symbols are mapped into frequency and spatial domain to make advantage of diversity offered by multiple spatial channels. In case of uncorrelated channels, the probability that all of them are in deep fade is much lower than the probability of just one channel being in fade. Thus, antenna correlation is not desired for SFBC transmission.

For the original source, please see [12]. But the truth is, SFBC is an application of older idea, space-time block coding (STBC). STBC uses time and spatial domain in the same manner as described above. Shift into frequency domain became logical after widespread adaptation of OFDM. The original and most famous STBC was published in [13], but since then, a lot of other literature is available. For quite thorough STBC analysis, [14] is a good example.

3.2.1 SFBC definition

Because SFBC are block-based codes, they operate on a fixed number of subcarriers. In LTE, the scheme is defined for two and four transmit antennas and they work on two and four subcarrier basis, respectively. A transmitter and receiver structure for two transmit and one receive antennas is shown in Figure 3.3. Again, each transmit antenna has its own IDFT block, and the spatial coding is preceding it. In the receiver, CP removal is followed by DFT and spatial decoding.

The equation-wise definition of SFBC procedure can be found in [7]. We will define it here in a more convenient way, both for two and four transmit antennas. The former definition is given in equation (3.10) and the latter in (3.11). The equation (3.10) is valid for the same system as depicted in Figure 3.3. Additive noise should be present on RHS, but for the convenience we will not include it.

$$\begin{bmatrix} y_0 \\ y_1 \end{bmatrix} = \begin{bmatrix} x_0 & -x_1^* \\ x_1 & x_0^* \end{bmatrix} \begin{bmatrix} h_{01}^{(0)} \\ h_{01}^{(1)} \end{bmatrix} \tag{3.10}$$

$$\begin{bmatrix} y_0 \\ y_1 \\ y_2 \\ y_3 \end{bmatrix} = \begin{bmatrix} x_0 & 0 & -x_1^* & 0 \\ x_1 & 0 & x_0^* & 0 \\ 0 & x_2 & 0 & -x_3^* \\ 0 & x_3 & 0 & x_2^* \end{bmatrix} \begin{bmatrix} h_{02}^{(0)} \\ h_{13}^{(1)} \\ h_{02}^{(2)} \\ h_{13}^{(3)} \end{bmatrix} \tag{3.11}$$

Transmitted symbols are denoted by x and received symbols by y. Elements $h_{01}^{(0)}$ and $h_{01}^{(1)}$ are channel coefficients on subcarrier 0 and 1 (subscript indeces) belonging to antennas 0 and 1, respectively (superscript indeces). We use indeces 0 and 1, but the same equation applies for every subcarrier pair, by changing 0 to $2i$ and 1 to $2i+1$. In STBC, the channel should not change during the time interval of one block (two symbols for Alamouti code [13]). In the same manner, for SFBC, channel should remain constant on the set of subcarriers where the block is applied.

LTE's SFBC can also be written by means of equivalent channel $\mathbf{H}_{eq}$. The two transmit antenna version is given here:

$$\begin{bmatrix} y_0 \\ y_1^* \end{bmatrix} = \begin{bmatrix} h_{01}^{(0)} & -h_{01}^{(1)} \\ h_{01}^{(1)*} & h_{01}^{(0)*} \end{bmatrix} \begin{bmatrix} x_0 \\ x_1^* \end{bmatrix} = \mathbf{H}_{eq} \begin{bmatrix} x_0 \\ x_1^* \end{bmatrix}. \tag{3.12}$$

For SFBC decoding, we can either use maximum ratio combining (3.13) presented in original STBC paper, or, thanks to linear model with $\mathbf{H}_{eq}$, we can deploy classical equalizer like LMMSE (3.5). Both approaches are applicable also for multiple receive antennas, in which case matrix $\mathbf{H}_{eq}$ and vector with received samples y would be taller accordingly.

$$\begin{bmatrix} r_0 \\ r_1 \end{bmatrix} = \begin{bmatrix} h_{01}^{(0)*} & h_{01}^{(1)} \\ h_{01}^{(1)*} & -h_{01}^{(0)} \end{bmatrix} \begin{bmatrix} y_0 \\ y_1^* \end{bmatrix} = \begin{bmatrix} x_0 \left(|h_{01}^{(0)}|^2 + |h_{01}^{(1)}|^2 \right) \\ -x_1^* \left(|h_{01}^{(0)}|^2 + |h_{01}^{(1)}|^2 \right) \end{bmatrix} \tag{3.13}$$

3.2.2 SFBC performance simulations

Again, we present basic BER simulation results. Unlike with CDD, SFBCs do not need channel coding to improve the performance, which made the script a bit simpler. System parameters are summarized in following list:

- OFDM transmission with 512 FFT bins, 300 are used.
- Block fading with one channel realization per OFDM symbol.
- QPSK modulation, no channel coding.
- Frequency flat Rayleigh channel.

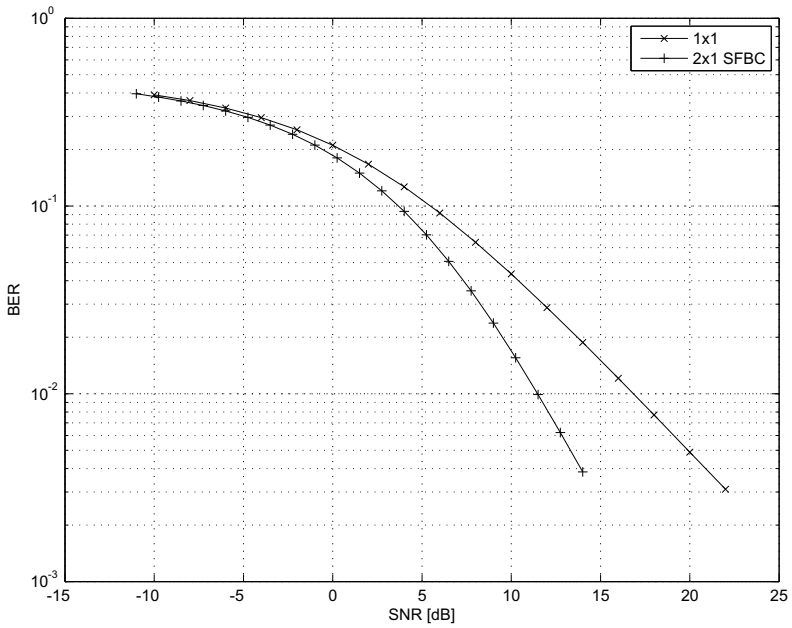

Figure 3.4 *Bit error rate curve for SFBC*

- FDE LMMSE receiver with full channel knowledge.
- Unit power per used FFT bin.

Performance plots are shown in Figure 3.4. There are results for SISO system and 2x1 SFBC system. We also simulated 4x1 SFBC version and the results proved our earlier claim. The same diversity order has led to same BER performance. It does not hold with channel coding present. In that case four antenna version performs a bit worse in low SNR region but quite better in higher SNRs. Generally, we can see that the scheme performs very well. STBCs and SFBCs generally give better results than CDD, they are helpful also when frequency selectivity is already present.

3.3 Open-loop spatial multiplexing

In order to have an option of multi-layer transmission without having any CSI at the transmitter, a scheme described in this section has been included in [7]. The algorithm can be described as a combination of layer transformation, cyclic delay diversity and precoding with statically selected weighting matrix.

Definition is based on

$$\begin{bmatrix} y^{(0)}(k) \\ \vdots \\ y^{(N_t-1)}(k) \end{bmatrix} = \mathbf{W}(k)\mathbf{D}(k)\mathbf{U} \begin{bmatrix} x^{(0)}(k) \\ \vdots \\ y^{(\nu-1)}(k) \end{bmatrix}, \tag{3.14}$$

Number of layers ν	$\mathbf{U}$	$\mathbf{D}(k)$
2	$\frac{1}{\sqrt{2}}\begin{bmatrix} 1 & 1 \\ 1 & e^{-j2\pi/2} \end{bmatrix}$	$\begin{bmatrix} 1 & 0 \\ 0 & e^{-j2\pi k/2} \end{bmatrix}$
3	$\frac{1}{\sqrt{3}}\begin{bmatrix} 1 & 1 & 1 \\ 1 & e^{-j2\pi/3} & e^{-j4\pi/3} \\ 1 & e^{-j4\pi/3} & e^{-j8\pi/3} \end{bmatrix}$	$\begin{bmatrix} 1 & 0 & 0 \\ 0 & e^{-j2\pi k/3} & 0 \\ 0 & 0 & e^{-j4\pi k/3} \end{bmatrix}$
4	$\frac{1}{2}\begin{bmatrix} 1 & 1 & 1 & 1 \\ 1 & e^{-j2\pi/4} & e^{-j4\pi/4} & e^{-j6\pi/4} \\ 1 & e^{-j4\pi/4} & e^{-j8\pi/4} & e^{-j12\pi/4} \\ 1 & e^{-j6\pi/4} & e^{-j12\pi/4} & e^{-j18\pi/4} \end{bmatrix}$	$\begin{bmatrix} 1 & 0 & 0 & 0 \\ 0 & e^{-j2\pi k/4} & 0 & 0 \\ 0 & 0 & e^{-j4\pi k/4} & 0 \\ 0 & 0 & 0 & e^{-j6\pi k/4} \end{bmatrix}$

Table 3.1 *Layer transformation and CDD matrices for open-loop spatial multiplexing*

where $x^{(0)} \dots x^{(\nu-1)}$ are input symbols on ν layers, $\mathbf{U}$ is a $\nu \times \nu$ layer transformation DFT matrix, $\mathbf{D}$ is a diagonal $\nu \times \nu$ CDD matrix, $\mathbf{W}$ is a $N_t \times \nu$ precoding matrix, $y^{(0)} \dots y^{(N_t-1)}$ are output symbols on N_t antennas and k is a subcarrier index.

Matrices $\mathbf{U}$ and $\mathbf{D}$ for all possible numbers of layers ν are presented in Table 3.1. Precoding matrices $\mathbf{W}$ are taken from the codebook used in case of closed-loop precoding (Section 3.5). With two transmit antennas, only matrix with index 0 is used. For four antennas, the transmitter periodically changes matrices with indeces 12-15 according to equation

$$i = \mathrm{mod}\left(\left\lceil \frac{k+1}{\nu} \right\rceil - 1, 4\right) + 13. \tag{3.15}$$

In both cases the behavior is predetermined, therefore no feedback is needed. Now when the scheme is defined, we will present simulation results of an ideal system with two and four transmit antennas and two receive antennas. As we use spatial multiplexing scheme, we will use theoretical relative throughput as performance measure. This throughput is calculated from the number of successfully received Turbo codewords, with theoretical maximum set to one. Erroneous codewords would have to be retransmitted. The results can be found in Figure 3.5. We included also 2x2 SFBC scheme for comparison. We can see that periodically changing precoding matrices has worse performance in low SNR region. Nevertheless, it is an area where SFBC would be preferred. In higher SNR region the performance is superior. Simulation parameters are summarized in following list.

- OFDM transmission with 512 FFT bins, 300 are used.
- Block fading with one channel realization per OFDM symbol.
- QPSK modulation.
- 3GPP Turbo code with 1/2 ECR, one codeword per OFDM symbol, no interleaving.
- Frequency flat Rayleigh channel.
- FDE LMMSE receiver with full channel knowledge.
- Unit power per used FFT bin.

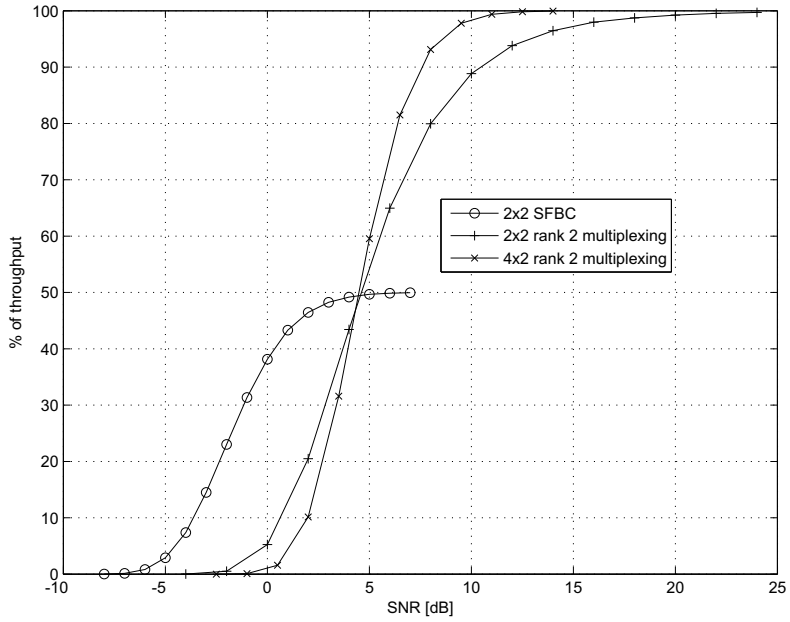

Figure 3.5 *Throughput curves of open-loop spatial multiplexing and SFBC systems.*

3.4 SVD-based precoding

This section's title is actually not used as an algorithm name by the research community. Though, it is a well known scheme, which is usually used to derive MIMO capacity with full CSI at the transmitter, or closed-loop capacity as called in [14]. CSI may be obtained by using feedback signalling or exploiting channel reciprocity, if possible. Unlike other algorithms described in this chapter, SVD-based precoding has never been included in 3GPP specifications. It has been considered, but simulations showed that small channel coherence bandwidth prevents efficient deployment into the system.

The idea behind this scheme is that by applying SVD (3.16), we can diagonalize the channel into $\min(N_t, N_r)$ parallel channels. In the equation, $\mathbf{V}$ is a $N_t \times N_t$ unitary 'transmit' matrix, Σ is a $N_r \times N_t$ matrix with $\min(N_t, N_r)$ singular values on the main diagonal and $\mathbf{U}$ is a $N_r \times N_r$ unitary 'receive' matrix.

$$\mathbf{H} = \mathbf{U}\ \Sigma\ \mathbf{V}^H \tag{3.16}$$

By using $\mathbf{V}$ as a transmit beam-forming matrix and $\mathbf{U}^H$ as a receive beam-forming matrix, we construct $\min(N_t, N_r)$ orthogonal and non-interfering parallel channels (modes). Gain of these channels is generally different and is given by eigenvalues of the channel. It can be seen from application on our signal model (3.17).

$$\mathbf{y} = \mathbf{U}^H\mathbf{H}\mathbf{V}\mathbf{x} + \mathbf{U}^H\mathbf{n} = \mathbf{U}^H\mathbf{U}\ \Sigma\ \mathbf{V}^H\mathbf{V}\mathbf{x} + \mathbf{U}^H\mathbf{n} = \Sigma\mathbf{x} + \mathbf{U}^H\mathbf{n} \tag{3.17}$$

Information about mode gains is useful also for lower rank transmissions. We already know that

maximum number of transmitted layers is $\min(N_t, N_r)$. If we choose to send lower amount of data, we use ν of N_t columns of $\mathbf{V}$ as our precoding matrix. The smart way is to take columns which belong to strongest singular values. In a single-layer case, only one column is chosen and the precoder performs ideal beam-forming, sending the layer into strongest channel mode.

With OFDM, a new dimension is added into SVD precoding. The typical cellular channel is frequency selective, resulting in different $\mathbf{H}_i$ matrix on each subcarrier. Perfect precoder would therefore apply appropriate $\mathbf{V}$ matrix for each FFT bin. This is quite an issue from implementation point of view, especially if the scheduling is based on resource blocks. A possible solution is applying single precoding matrix on a subset of subcarriers, according to equation (3.18). Here, SVD is applied on covariance matrix $\mathbf{R}_H$, which is averaged through given subcarriers. This inevitably leads to a tradeoff between performance and implementation complexity.

$$\mathbf{R}_{\mathrm{H}} = E\left[\mathbf{H}_i^H \mathbf{H}_i\right] = \mathbf{U}\ \Sigma\ \mathbf{V}^H \tag{3.18}$$

Getting close to MIMO channel capacity goes also hand to hand with spatial waterfilling. It is desired to transmit more power into stronger mode, but only to a point when it increases system throughput. If the mode is saturated (ceiling effect), rest of the power should be distributed into weaker modes. For this work, waterfilling is not considered. We simply accept $\mathbf{V}$ as the ideal precoding matrix.

3.4.1 Performance simulation

Basic link simulations are shown in this section. The first case evaluates uncoded bit error performance of system with ideal beam-forming for two and four antennas. Settings of the script are in following list:

- OFDM transmission with 512 FFT bins, 300 are used.
- Block fading with one channel realization per OFDM symbol.
- QPSK modulation, no channel coding.
- Frequency flat Rayleigh channel.
- FDE LMMSE receiver with full channel knowledge.
- Unit power per used FFT bin.

Results of the simulation are in Figure 3.6. SVD as an ideal beam-former does not disappoint, each added antenna provides quite significant performance gain.

Second simulation provides comparison between single-layer and multi-layer transmission. We used the same settings, added 3GPP Turbo code with effective code rate 1/2 and used theoretical relative throughput as a performance measure (same settings as in case of open-loop spatial multiplexing). This throughput is calculated from block error rate, where one block equals one OFDM symbol. Results are presented in Figure 3.7. We compare throughput curves of SISO system with single-layer and dual-layer MIMO system.

From the Figure we can nicely deduce a concept of *rank adaptation*. A smart transmitter would use the number of layers that would provide best throughput for given SNR value. In our case, it would be single-layer until approximately 8dB, and then the system would switch to dual-layer option.

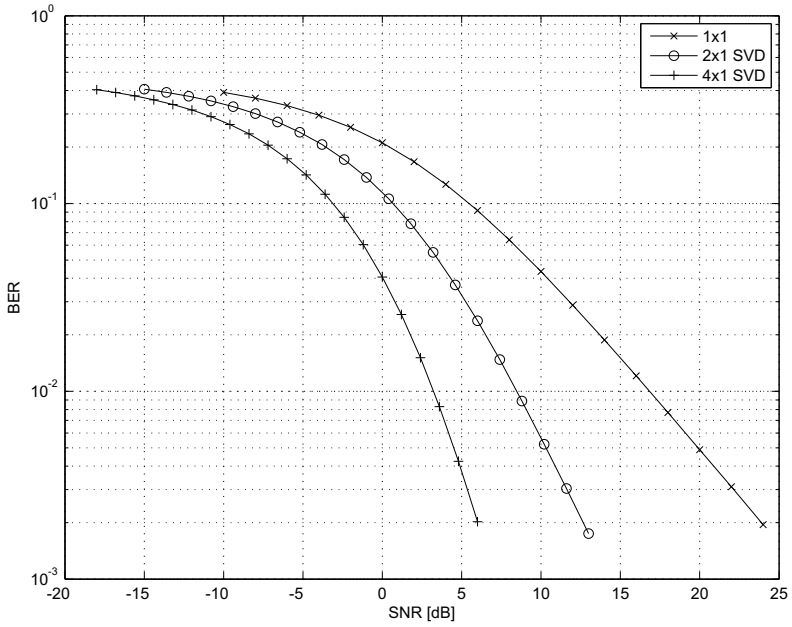

Figure 3.6 *Optimal beam-forming performance curves*

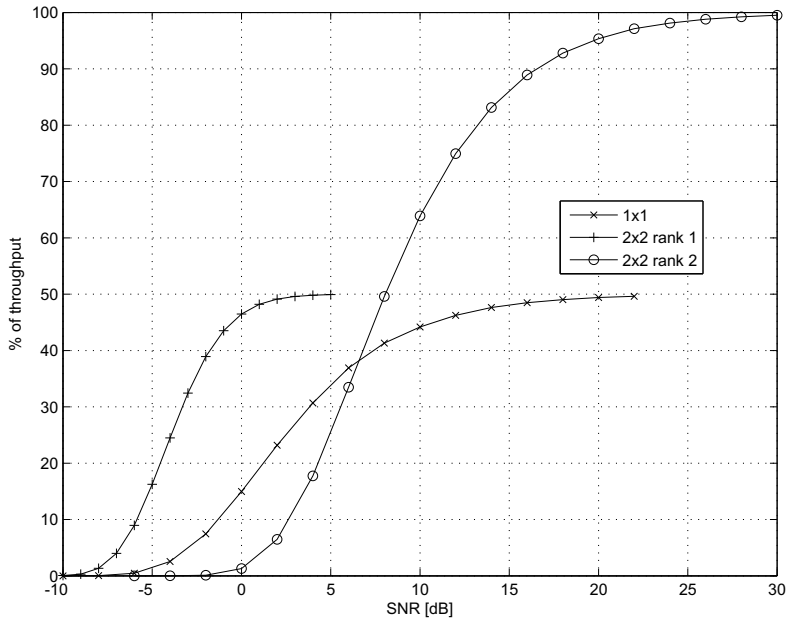

Figure 3.7 *Optimal precoding throughput curves*

3.5 Codebook-based precoding

In previous section we described an optimal way to precode symbols we want to transmit. We saw that there is one important and problematic requirement - the transmitter has to have full channel knowledge. Full CSI is naturally available only in ideally reciprocal channel, otherwise it must be provided by signalling. However, such a feedback would create particularly large overhead.

This section shortly presents a solution similar to vector quantization, which is a well known approach in image and video compression. We call it codebook-based precoding and it seems to be the most promising MIMO option in LTE's downlink. Codebook $\mathcal{W}$ is a set of indexed precoding matrices, from which the best one is selected by relatively small number of bits in feedback message. The scheme can be therefore defined as closed-loop precoding with partial CSI at the transmitter.

We compared the algorithm to vector quantization, because the basic idea of reporting just an index of quantized multi-dimensional value is identical. The codebook is a set of precoding matrices $\mathbf{W}_i$, which quantize the ideal matrix defined in Section 3.4. Logically, the more quantization bits we have available, the better the performance should be. But even with a small number of bits, the gain can be quite high. That is very practical, because designing robust feedback channel can consume a lot of resources.

In the same manner as in precoding with full CSI, using OFDM in frequency selective channel can lead to different optimal quantized precoding matrices on different subcarriers. Reporting a PMI for each of them would be impractical. However, dividing the allocated spectrum into subbands and using subband specific feedback is manageable. The gains can be significant, especially in urban channels with low coherence bandwidth.

Codeword selection

An important issue in codebook-based system is a metric, which serves for choosing the best precoding matrix $\mathbf{W}$ from available set $\mathcal{W}$. In case of beam-forming, by maximizing Frobenius norm of equivalent channel $\mathbf{H}_{eq}$ from our signal model (3.4), we maximize channel gain for given single-layer transmission. However, inter-layer interference in spatial multiplexing case makes choosing the optimal precoding matrix more complicated. A nice insight into the issue can be found in [15]. For linear receivers, there are two basic approaches - *Minimum Singular Value* and *Mean Squared Error* (MSV and MSE) selection criteria. In order to minimize bit error probability, we will use MSV criterion, which is defined according to

$$\mathbf{W} = \underset{\mathbf{W}_i \in \mathcal{W}}{\operatorname{argmax}} \lambda_{min} \left\{ \mathbf{H}\mathbf{W}_i \right\}, \tag{3.19}$$

where $\lambda_{min} \left\{ \mathbf{H}\mathbf{W}_i \right\}$ is a minimal singular value of given equivalent channel.

From previous work on the project we were also provided by algorithm specifically useful when using rank adaptation. Step-by-step description is given in following list. Note that it can perform codeword selection from codebooks belonging to all possible amounts of layers, choosing ν that gives highest performance.

1. For given channel and precoding matrices, we compute equivalent channel $\mathbf{H}_eq$.
2. We consider LMMSE receiver, where $\mathbf{G}_{LMMSE} = \left(\mathbf{H}_{eq}^H \mathbf{H}_{eq} + \sigma^2 \mathbf{I} \right)^{-1} \mathbf{H}_{eq}^H$.

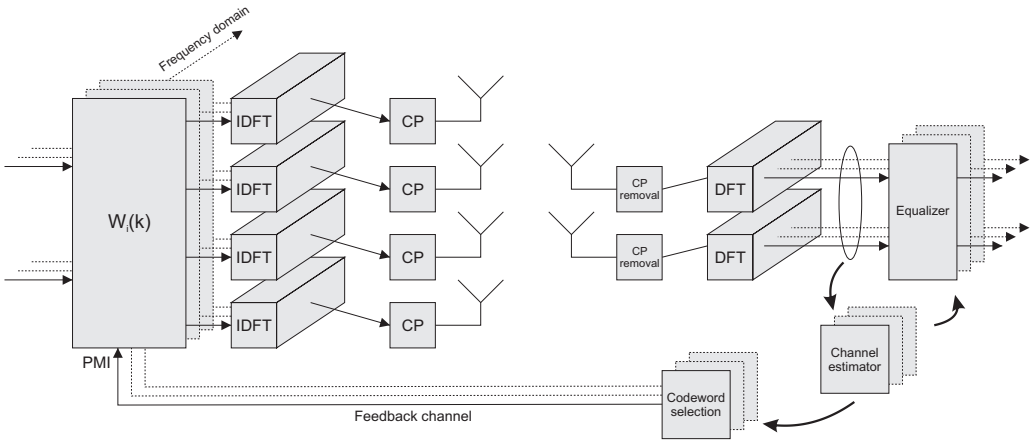

Figure 3.8 *Closed-loop system block diagram*

3. Given the receiver weighting matrix, we calculate SINR for each layer.
4. Obtained ratios are then mapped into input/output mutual information, using pre-computed curve for given MCS.
5. Mutual informations are mapped into theoretical single-layer throuhgputs. For that, we use throughput curves modeled by hyperbolic tangent functions. Parameters of these curves are obtained by simulating single-layer transmission using given MCS and flat fading channel, and stored in the memory.
6. Throuputs of all layers are summed.
7. We repeat steps 1 to 6 for each precoding matrix from the codebook and use the one that results in highest theoretical throughput.

3.5.1 Definition of LTE's closed-loop MIMO scheme

In this section we present proper definition of codebook-based MIMO precoding, as given by 3GPP specification. To get a closer insight, in Figure 3.8 we also provide basic block diagram. It is a 4x2 MIMO system example with no requirements on channel reciprocity (FDD). On each subband, the transmitter applies precoding matrix $\mathbf{W}_i$ and thus spreads symbol from given layers over all transmit antennas. On the receiver side, the system uses channel estimation algorithms to obtain channel knowledge and calculate best $\mathbf{W}_i$ from codebook $\mathcal{W}$.

In older versions of [7], where short delay CDD was allowed, precoding was defined by equation (3.8). By removing CDD matrix we get equation valid for the latest specification:

$$\begin{bmatrix} y^{(0)}(k) \\ \vdots \\ y^{(P-1)}(k) \end{bmatrix} = \mathbf{W}(k) \begin{bmatrix} x^{(0)}(k) \\ \vdots \\ x^{(\nu-1)}(k) \end{bmatrix}, \tag{3.20}$$

where $x^{(0)}, \ldots, x^{(\nu-1)}$ are input symbols in ν layers, $y^{(0)}, \ldots, y^{(N_t-1)}$ are symbols transmitted from N_t antennas, $\mathbf{W}$ is a size $N_t \times \nu$ MIMO precoding matrix and k is a subcarrier index.

Codebook index	Number of layers ν	
	1	2
0	$\frac{1}{\sqrt{2}}\begin{bmatrix}1\\1\end{bmatrix}$	$\frac{1}{\sqrt{2}}\begin{bmatrix}1 & 0\\0 & 1\end{bmatrix}$
1	$\frac{1}{\sqrt{2}}\begin{bmatrix}1\\-1\end{bmatrix}$	$\frac{1}{2}\begin{bmatrix}1 & 1\\1 & -1\end{bmatrix}$
2	$\frac{1}{\sqrt{2}}\begin{bmatrix}1\\j\end{bmatrix}$	$\frac{1}{2}\begin{bmatrix}1 & 1\\j & -j\end{bmatrix}$
3	$\frac{1}{\sqrt{2}}\begin{bmatrix}1\\-j\end{bmatrix}$	-

Table 3.2 *Codebook for transmission on two antennas*

System bandwidth N_{RB}^{DL}	Subband size
6 - 7	(wideband CQI/PMI/RI only)
8 - 10	4
11 - 26	4
27 - 63	6
64 - 110	8

Table 3.3 *Subband granularity*

In Table 3.2 we present LTE's codebook for two transmit antennas. It is rather small, requiring only two feedback bits per subband. Two codewords performing antenna selection were also present in [7] before version 8.3.0, but were removed for implementation issues afterwards. For four-antenna codebook, we refer to the specification. It contains 16 codewords for each number of layers, thus requiring four feedback bits per subband. Implementation issues pressed LTE into using constant-modulus codewords, keeping symbol energy per antenna constant.

LTE's subband granularity is presented in Table 3.3. There are different modes in which CQI, PMI and RI can be reported. Usually, UE sends *wideband* information periodically, and subband corrections can optionally be sent when needed. Subband size depends on system bandwidth and is defined by number of resource blocks per subband.

3.5.2 Basic simulations

In the usual manner, we conclude closed-loop section by showing basic simulation results. We present BER curves for beam-forming in Figure 3.9 and theoretical relative throughput curves for spatial multiplexing in Figure 3.10. Both plots contain SISO case for comparison. Simulation parameters are summarized in the following list:

- OFDM transmission with 512 FFT bins, 300 are used.

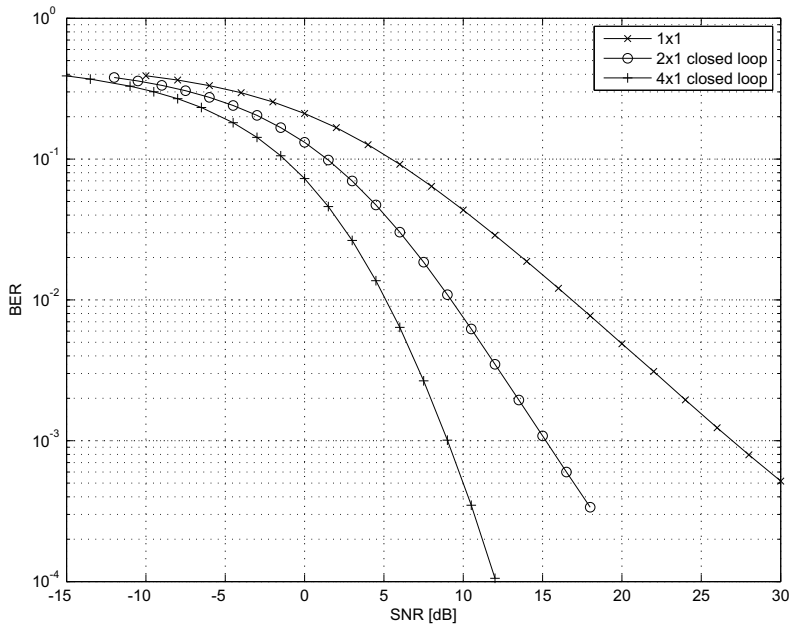

Figure 3.9 *Performance curves of closed-loop beam-forming with LTE codebook*

- Block fading with one channel realization per OFDM symbol.
- QPSK modulation.
- No channel coding for beam-forming, 3GPP Turbo code with 1/2 ECR and single codeword per OFDM symbol for spatial multiplexing.
- Codeword selection by Frobenius norm for beam-forming, MSV for spatial multiplexing.
- Frequency flat Rayleigh channel.
- FDE LMMSE receiver with full channel knowledge.
- Unit power per used FFT bin.

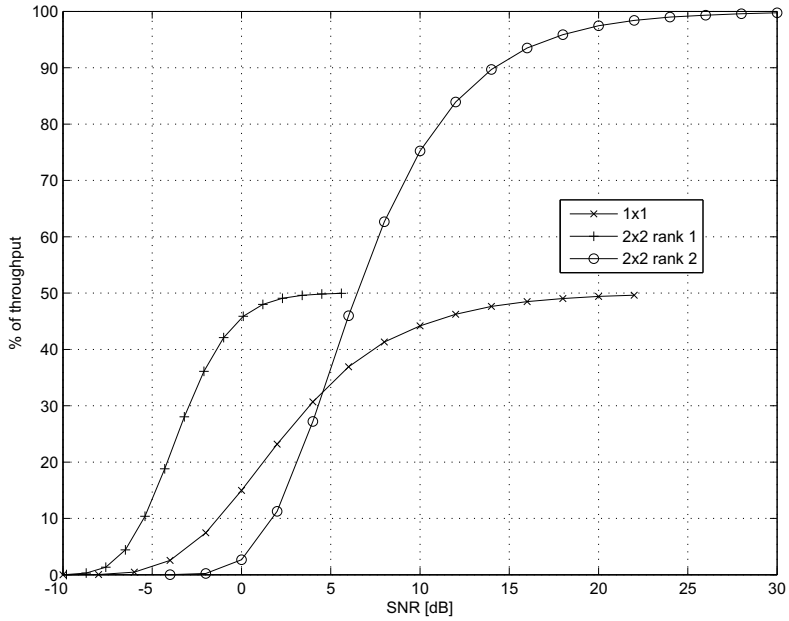

Figure 3.10 *Comparison of throughput for 2x2 MIMO system with LTE codebook*

Chapter 4

Research contribution

We introduce the last and the most important chapter of our work. We have described LTE, the outcome of long and hard work, with putting special attention to MIMO transmission schemes in downlink. Now it is time to start following our assignment. We will take these algorithms, insert them into uplink processing chain, and model this system in wideband local area channel. We will try to find out how much additional gain can be expected in single-layer transmission, and how would a potential spatial multiplexing scheme perform.

The chapter will start with a short insight into system changes that would be necessary, if MIMO is taken into account. Channel estimation gets some attention, because its performance can be improved in low mobility scenario, which is expected in local area environment. After that, the modelling platform that we used is described. We will address the simulator structure, method for modelling given wireless channel, and numerology choice for our hypothetical uplink channel. The platform is then used firstly for analysing behavior of indoor channel, and secondly for studying performance of given MIMO algorithms in it. Finally, in the last two sections, we will pursue further possibilities provided by TDD and study impact of used schemes on PAR of the transmitted signal.

4.1 MIMO related system changes

Deploying multi-antenna transmission schemes into an existing system does not come for free. Most obviously, for all the previously mentioned algorithms, the mobile station will need to be equipped with multiple RF chains, including power amplifiers. This automatically leads to increased production cost and power consumption, therefore the deployment should not be mandatory. As a mid-step alternative, there is an option of having one RF chain which could switch between multiple transmit antennas, implying an antenna selection diversity scheme, but we will not consider this in our work.

Looking at the standardization process beyond LTE, it is not clear if the requirements for uplink spectral efficiency can be met with two transmit antennas (providing maximum of dual layer transmission). Some companies already want to have a possibility of having four transmit antennas in the mobile station. However, for this work, we will consider deployment of two transmit antennas. Extending the conclusions for four or more transmit antennas would be straightforward.

All of the considered algorithms require changes in the transmitter and receiver. Additionally, closed-loop scheme needs feedback signalling, and optimal precoding requires CSI at the transmitter. The feedback information can be carried by downlink control channel, which means that format of the controlling messages will need to be redefined. As for the SVD-based precoding, the deployment only makes sense in TDD scenario, where channel reciprocity is available.

Another issue coming up with deployment of multiple transmit antennas is reference signal structure. The receiver needs to know the complete channel matrix **H**. In most of the cases, this means that each antenna should transmit different, orthogonal pilot signal. Orthogonality ensures that these sequences, and therefore also channel estimation, can be separated in the receiver. A bit different approach has to be pursued with optimal precoding. The precoding matrix is only known at the transmitter and the best way to pass the information to the receiver is to apply it also on reference signal. Therefore, instead of having orthogonal sequences for each transmit antenna, we would need an orthogonal sequence for each transmission layer.

Channel estimation

This work definitely does not aim to provide analysis of channel estimation in hypothetical MIMO uplink system. However, one part of the assignment is to evaluate influence of low mobile station mobility on the performance. Low mobility suggests that our wireless channel will not change fastly in time. This can be picked up for example by lowering signalling control overhead, as CSI/PMI/RI would not have to be reported as often as in high mobility scenarios. On the other hand, we can use time smoothing to increase precision of channel estimation, which would actually lead to increased system performance. It would not be always possible, as subsequent time domain resources may not be assigned to the same user, but the possibility is here. To give an exemplary demonstration, we will use a channel estimation algorithm suggested by the research team, make necessary changes to deploy it in MIMO system and simulate influence on time smoothing in local area scenario.

We will start with a brief description of channel estimation algorithm we were provided with. It is a data-aided approach, based on equations 14-30 to 14-36 from [16]. In the book, the estimator is meant for application in time domain, however we use it optionally in time and always in frequency domain, in this order. It is a two step approach, where at first ML estimates on available resource elements are calculated, and then Wiener smoothing is applied in given domain. The smoothing is based on autocorrelation function. In frequency domain, this function is pre-simulated, because obtaining an analytical expression is not a trivial task. In time domain, it is calculated from classical Jakes model with Doppler shift. We do not want to go into details here, the only detail we need to know is that as the first step the ML estimate is calculated by multiplying the received pilot signal in frequency domain with the complex conjugate of the original pilot signal. It is an operation equivalent to correlating the sequences in time domain.

Now, to apply the algorithm on two transmit antennas, we needed to modify the ML step. We took the first possible Zadoff-Chu sequence as a pilot signal for the first antenna, and time cyclic shifted version of the same seqeuence as a pilot signal for the second antenna. We chose the cyclic shift value to be exactly half of the sequence's length, which allowed us to perform a little trick while obtaining the mentioned ML estimate. If we have a frequency domain pilot sequence

$$A^{(1)} = [a_0, a_1, a_2, a_3, \ldots, a_{N-1}]^T, \tag{4.1}$$

after half length time domain cyclic shifting, the sequence for the second antenna is

$$A^{(2)} = [a_0, -a_1, a_2, -a_3, \ldots, a_{N-1}, -a_{N-1}]^T . \tag{4.2}$$

For the sake of example, we consider 2x1 system and show the approach on the first two subcarriers. For next step we need to make one crucial assumption - we consider the channel to remain constant on two subsequent subcarriers. For indoor channels this is not a problem, but it may not be true in general. The received reference symbols on first two subcarriers will be

$$\begin{aligned} r_0 &= a_0 h_{01}^{(1)} + a_0 h_{01}^{(2)} = a_0 \left(h_{01}^{(1)} + h_{01}^{(2)} \right) \\ r_1 &= a_1 h_{01}^{(1)} - a_1 h_{01}^{(2)} = a_1 \left(h_{01}^{(1)} - h_{01}^{(2)} \right) \end{aligned} . \tag{4.3}$$

By multiplying the received pilots with complex conjugates of original unshifted sequence, we get

$$\begin{aligned} z_0 &= r_0 a_0^* = |a_0|^2 \left(h_{01}^{(1)} + h_{01}^{(2)} \right) = \tfrac{1}{2} \left(h_{01}^{(1)} + h_{01}^{(2)} \right) \\ z_1 &= r_1 a_1^* = |a_1|^2 \left(h_{01}^{(1)} - h_{01}^{(2)} \right) = \tfrac{1}{2} \left(h_{01}^{(1)} - h_{01}^{(2)} \right) \end{aligned} . \tag{4.4}$$

The power of reference symbols is normalized to $\frac{1}{N_t}$, in the same manner as user data symbols. The results can already be combined into our new ML estimates

$$\begin{aligned} \hat{h}_{01}^{(1)} &= z_0 + z_1 \\ \hat{h}_{01}^{(2)} &= z_0 - z_1 \end{aligned} . \tag{4.5}$$

We omitted the noise term for simplicity. The approach is then repeated for all subcarrier pairs. After this step, time and frequency Wiener smoothing can be applied, in the same way as with single transmit antenna. To conclude the insight, in Figure 4.1 we present performance comparison of channel estimator with one and two antennas. As the reference sequence power is lower in multi-antenna case, we would expect the estimation to perform worse in the whole region. However, it is not so. Low SNR surpresses the difference.

4.2 Introduction to simulations

In Chapter 3, basic performance simulation results of several MIMO transmission schemes were already presented. Those plots have mostly illustrative purposes. At this point however, simulation results are the important part, following the actual task of this work. Simulating performance and different influences using relevant system model should show us, whether deploying multiple transmission antennas in mobile station is the right way to go. Therefore, we will spend some time here describing our modelling approach.

All the simulations in this work are based on Monte Carlo methods. Knowing the statistical properties, we create large amount of random wireless channel realizations and evaluate our system's performance in it. The transmission is modeled in baseband, creating random user bits, applying transmission algorithms, MIMO channel and receiver algorithms. With enough random realizations, we expect to get smooth performance curves. For these purposes, a single simulation platform has been created, details being explained in section 4.2.1.

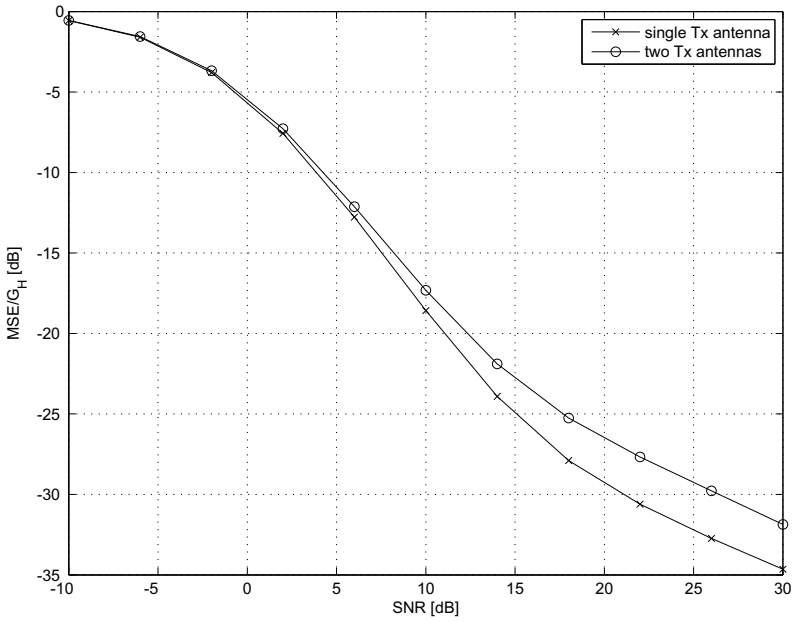

Figure 4.1 *Channel estimator performance*

General settings

Our simulator is based on LTE's time domain resource called slot. For each such slot, one MIMO channel realization is generated, and it stays constant during this slot. This kind of approach is called block fading. While wireless channel genarally changes in time domain, in local area environment with low mobile station velocities the block fading model can be justified well. Now that we mentioned time domain settings, we note that our simulator uses combination of LTE and local area optimized numerology, with further details specified in section 4.2.2.

As we are aiming for evolution based on LTE, time/frequency numerology is not the only part of the settings where we draw inspiration from it. Multiplexing scheme, channel coding and interleaving and other options in our simulations are by default taken from LTE specifications. In the following list, we summarize most of the important settings. Some of them are used all the time, some need to be changed in some cases. Those changes will be highlighted when results of such simulations are presented.

- We will simulate different multi-antenna transmission schemes. In order to provide fair comparison with performance of single transmit antenna system, overall transmission power (summed through all transmit antennas) will stay constant in all cases. As for the receiver, our simulations will consider four receive antennas.
- We will use SC-FDMA, unless otherwise stated. Keeping in mind that all LTE's MIMO steps are done in frequency domain, in our uplink simulations they are placed between DFT and IDFT transformations at the transmitter and receiver. This naturally affects the beforementioned 'single carrier' property, as will be analysed later. Most of the times, full

bandwidth transmission (see section 4.2.2) will be modelled, but there are also cases when smaller user bandwidth gets us to some conclusions.

- As a channel code, LTE's Turbo code with basic code rate 1/3, minimum and maximum block size 40 and 5000 bits respectively, is used. Its basic structure was mentioned in section 2.3.2, thorough definition can be found in [6]. Each block has 16 CRC tail bits attached at the end. Wide range of ECRs is supported, we will use those specified in [8] for LTE. Channel decoder uses an iterative Max-log-MAP algorithm, with number of iterations set to 8. Block based interleaving, also specified in [6], is used all along.
- We mostly use A1 NLOS scenario as a channel model. Details can be found in section 4.2.3. In terms of channel gain, NLOS version of A1 indoor channel is less favourable. By default, mobile station velocity is set to 3km/h, center frequency is 4GHz, and mobile station and base station antenna distances are set to 0.5λ and 50λ, respectively.
- By default, we use ideal channel estimation and ideal channel knowledge at the transmitter (in scenarios where needed). Changes in these settings will be again clarified, when necessary.

Now a few words about the things we do not model. From a system point of view, probably the most important omitted feature is hybrid-ARQ. It is a retransmission scheme (described in Section 2.1.1), it can however also lead to capacity improvement. Including hybrid-ARQ in our simulation platform would complicate things a lot. For MIMO algorithms, we generally do not simulates errors in feedback or CSI at the transmitter. These are problems that influence the performance generally, not only in local area deployment. Next, as we use a baseband model, phenomena related to carrier frequency, carrier phase or timing errors at the receiver will not be considered.

Performance measure

In all following simulations, throughput will be used as performance measure. This throughput will be measured in user bits per subcarrier, thus taking into account ECR of used channel code. That is the main reason why we used this metric. It provides a possibility of fair comparison between transmissions with different code gains.

4.2.1 Simulator structure

For all link performance simulations, a single flexible simulation platform has been created. Majority of the code is written in Matlab, only channel coding related functions are written in C language. In the following lines we will describe important features and structural details of the simulator.

Features

A wide range of system scenarios is supported by our simulation platform. Details are always defined at the beginning of the code, as different settings may use different files or functions. We summarized all possible settings into this list:

- *MIMO options:* One, two or four transmit antennas and any number of receive antennas can be used. Supported transmission schemes are:

  - **Receive diversity:** The basic scheme with one tranmit antennas.
  - **SFBC:** LTE's space-frequency block codes .
  - **CDD:** Cyclic delay diversity, recently removed from 3GPP specifications.
  - **Open-loop spatial multiplexing:** LTE's scheme described in section 3.3.
  - **Codebook-based closed-loop:** LTE's principal beamforming and spatial multiplexing scheme. The codebook from LTE can be changed for any other option. Combination with CDD, user specified precoding subband size and different codeword selection metrics (throughput, FN, MSV and MSE) are supported.
  - **SVD-based precoding:** Optimal beamforming and spatial multiplexing. Combination with CDD, user specified precoding subband size, option to use constant modulus codeword and RF chain imperfections modelling (see Section 4.4.2) are supported.

  All spatial multiplexing schemes can be used either with single or dual Turbo codewords. Closed-loop and optimal precoding schemes were also intended to support rank adaptation. However, because of memory leak problem during dynamic Turbo code initialization, this feature does not work reliably at this stage.
- *Numerology options:* In order to have flexible numerology possibilities, FFT size, subcarrier spacing, number of OFDM symbols in time slot, number of subcarriers per resource block, number of used resource blocks, offset of resource blocks placement in OFDM symbol and cyclic prefix length values can be specified by user.
- *MCS options:* BPSK and QPSK modulations are supported. Functions for 16QAM and 64QAM are included, however, these options do not run reliably at this stage. Turbo code from LTE with wide range of ECR can be used.
- *Channel parameters:* AWGN, frequency flat Rayleigh and WINNER II channel models are included in the implementation. In case of WINNER model, the user can further specify deployment scenario, center frequency, mobile station velocity, LOS/NLOS option and antenna distances on mobile and base stations.
- *Channel estimation:* Estimation can either be set to ideal, or to algorithm described in section 4.1. For the latter option, user can specify number of slots for time smoothing, and whether to estimate also noise power. Because of LTE's pilot structure and limitations of our estimation scheme, real channel estimation can only be used for one or two transmit antennas and 12 subcarriers wide resource blocks.

Structure

In this part of the section, we present block-by-block description of our simulation script. Some parts of the code were generally available, some were given to us by Nokia/NSN research team, and the rest we developed ourselves. Block diagram of the whole script is given in Figure 4.2. In the following list, all blocks are listed and described.

- *Set input parameters:* In the very beginning, parameters that set features described in previous part of the section have to be set.
- *Initializations:* The second block takes the input parameters, computes some secondary ones and prepares several necessary structures: constellation , throughput metric (if used), channel coding and interleaving (if rank adaptation is not used), pilot sequences and channel estimation filters (if used).

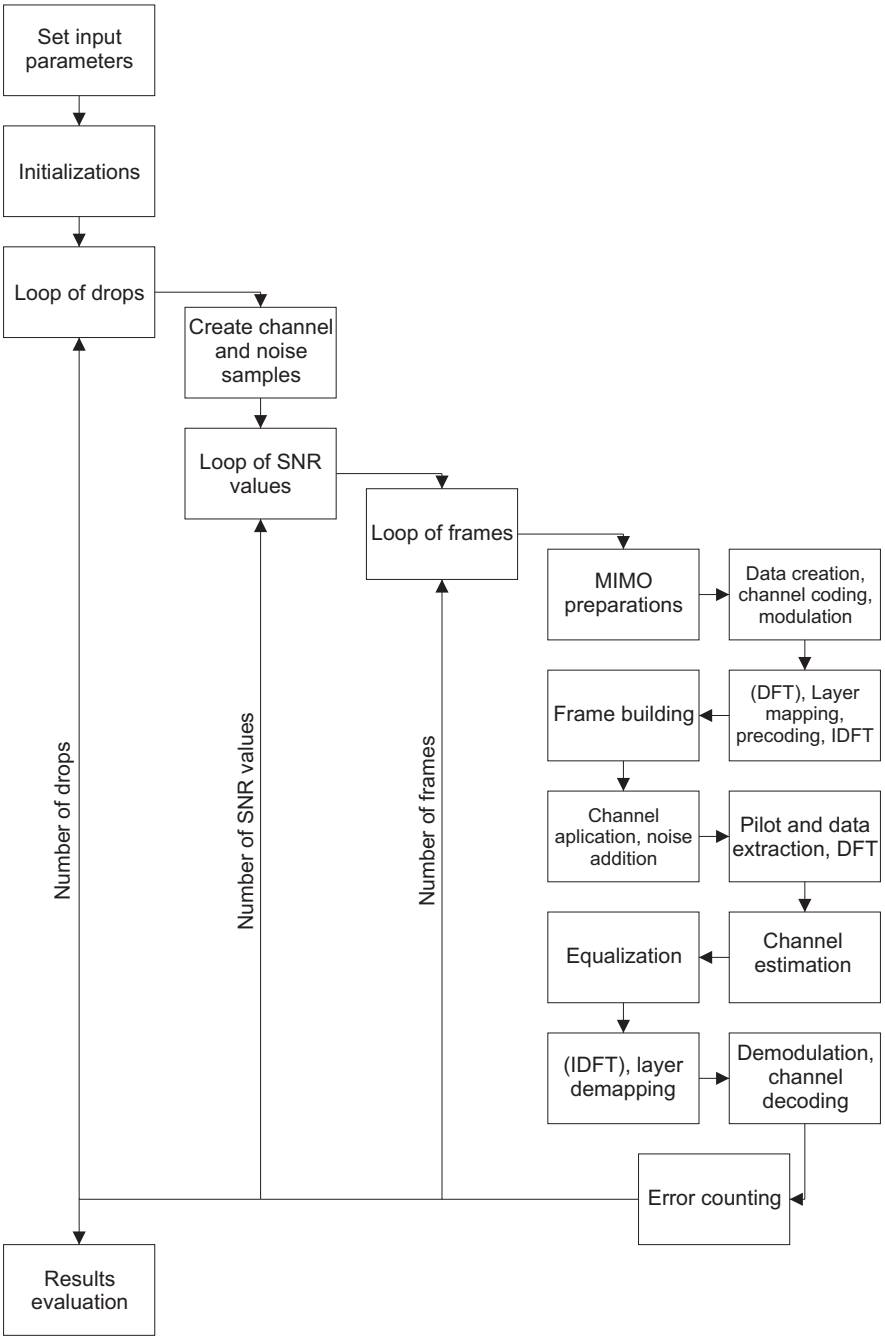

Figure 4.2 *Structure of used simulator*

- *Loop of drops:* Drops are scenarios with uncorrelated channel conditions. Channel realizations of different drops are i.i.d.
- *Channel and noise samples creation:* In this block channel and noise samples for all frames are created. Channel realizations for set of frames are given by time evolution of one scenario.
- *Loop of SNR values:* In order to get proper performance curves, a loop of user defined SNR values is provided. For all values the same noise samples are used, only the noise power is adjusted accordingly.
- *Loop of frames:* The main inner loop, where all interesting modelling is done. For each pass of the loop, one data slot (half of LTE's subframe) is created and its transmission simulated.
- *MIMO preparations:* For those MIMO schemes that require channel knowledge, preparation step is done in this block. In case of optimal precoding, matrices are calculated from SVD and in case of closed-loop scheme, PMI is chosen. If rank adaptation is on, also RI is chosen here.
- *Data creation, channel coding and modulation:* In this block, random data is created, encoded by Turbo channel coder, interleaved and then modulated. In case of rank adaptation, channel coder block settings are calculated dynamically according to already available RI values. However, the mentioned memory leak problem has to be kept in mind.
- *(DFT), layer mapping, precoding and IDFT:* If SC-FDMA is used, modulated data are transformed by DFT in the beginning of this block. After that, symbols are mapped into number of available layers, MIMO precoding is applied (if used), and symbols are shifted into time domain. At the end, cyclic prefix is placed in the beginning of each OFDM symbol.
- *Frame building:* In this block, an LTE slot is created from provided data and pilots.
- *Channel application and noise addition:* MIMO channel is applied here, using convolution. From N_t transmitted slots, N_r received slotes are calculated by summation. Then, noise samples are added.
- *Pilot and data extraction, DFT:* Here, the received samples are shifted into frequency domain. After that, pilots and data are extracted for separate processing.
- *Channel estimation:* In case of real channel estimation, received pilots, transmitted pilots and estimator filters are used here to obtain a channel estimate. If ideal channel estimation is set, receiver uses channel directly from channel sample generation step.
- *Equalization:* MIMO LMMSE equalization is performed in this block.
- *(IDFT), layer demapping:* If SC-FDMA was used, recieved symbols are transformed by IDFT. After that, layer demapping into one or two symbol streams is performed (according to the number of used Turbo coders).
- *Demodulation and channel decoding:* In this block, received symbols are finally demodulated, de-interleaved and decoded.
- *Error counting:* At the end of the loop, we compare transmitted and received coded and uncoded bits to count transmission bit errors. Also CRC bits are checked to count Turbo block errors.
- *Results evaluation:* With all simulations done and errors counted, the results are summarized into RBER, BER, BLER and throughput values, which can be then used for performance plots.

CP length	400ns ∼ 49 samples				
FFT size	512	1024	2048	4096	8192
CP overhead	8.73%	4.57%	2.34%	1.18%	0.59%
Subcarrier spacing [kHz]	240	120	60	30	15
Symbols per 1ms subframe	219	115	59	30	15

Table 4.1 *FFT options for 400ns long cyclic prefix*

CP length	1μs ∼ 123 samples				
FFT size	512	1024	2048	4096	8192
CP overhead	19.37%	10.72%	5.67%	2.92%	1.48%
Subcarrier spacing [kHz]	240	120	60	30	15
Symbols per 1ms subframe	194	107	57	29	15

Table 4.2 *FFT options for* 1μs *long cyclic prefix*

4.2.2 Local area optimized frame structure

Moving the research focus into wider bandwidths and higher carrier frequencies calls for substantial changes. A system 100MHz wide needs to be placed in higher part of the spectrum than available cellular networks. From availability point of view, especially 3.5GHz or 4GHz frequency bands come to mind. However, these bands require different treatment. Typically, path losses become larger with increasing carrier frequency , leading to significantly smaller cell sizes. Moreover, the propagation conditions are also expected to be different. Specifically, shorter power delay profile (larger coherence bandwidth) can be utilized in CQI/PMI/RI frequency domain granularities.

This section is mostly based on [17]. The main drivers behind local area-optimized numerology are possibility of shorter cyclic prefix overhead and need for larger subcarrier spacing. The former is due to short delay spread, while the latter would be preferred because of easier implementation of shorter FFT and worse phase noise condition in higher frequency bands. Also, increased number of subcarriers would lead to complexity increase of frequency domain channel estimation.

OFDM parameter options

As mentioned above, the length of CP needs to be reduced. Based on information from ITU, 3GPP and IEEE channel models, it was concluded that 400ns to 1μs CP should be sufficient for local areas. Shorter length reduces CP overhead, while longer CP could be usable for flexible spectrum usage (FSU), where different systems working next to each other in the spectrum can pick it up for synchronization purposes.

Sampling rate is also a parameter that needs to be optimized. However, in this case we are constrained, as a new generation local area terminal should stay compatible with legacy systems. Thus, it has to be a multiple of LTE's value. It was observed that selecting 122.88MHz, four times the sampling rate of LTE, is sufficient.

In Tables 4.1 and 4.2 we list possible OFDM settings, with 400ns and 1μs CP lengths. The

sample period, inverse value of 122MHz sampling rate, is 8.14ns. Especially FFT sizes of 1024 and 2048 bins seem promising. However, 1024 option would lead to dangerously small resource blocks, resulting in problematic design of reference symbols. From the other size, large FFT sizes offer very small CP overhead. Though, they also create long OFDM symbols, which is not desired for flexible TDD mode. With all the arguments summed, FFT size of 2048 with 60kHz subcarrier spacing becomes the preferred option.

Having the OFDM settings chosen, the next changes that come to mind are resource block properties. We will not go into details here, and again refer to [17]. The main drivers here are high data traffic, small number of users per cell and once again high coherence bandwidth. The two latter points support resource blocks larger in both time and frequency domain. Without going deeper, it is noted that preferred settings include subframe length of 0.5ms (29 OFDM symbols) and frequency band divided into 150 resource blocks, of which each occupies 10 subcarriers (600kHz).

In TDD mode, guard periods between downlink and uplink transmissions have to be taken into account. Counting with timing andvancement in uplink transmission and budgeting around 10μs for switching the circuitry from transmit to receive mode, it was concluded that the length of one optimized OFDM symbol (16.7μs) would be sufficient. Considering 5ms long frames, where each frame encapsulates 10 subframes times 29 OFDM symbols with 49 samples long CP, the system leaves us with

$$5ms - 10 \cdot 29 \cdot \frac{2048 + 49}{122.88\text{MHz}} = 51.03\mu\text{s}$$

for guard period purposes. It is roughly a size of additional three OFDM symbols. This time could be used as one long guard interval, but an alternate setting, allowing more frequent downlink/uplink switching, would divide it and place three shorter guard periods into the frame. The latter option is a preferred allocation strategy.

The situation in FDD is straightforward, as no additional intervals are needed. However, it would be beneficial, if the basic frame structure had the same basic settings as in TDD case, and also stayed friendly to LTE. Therefore, we keep the same settings as above and apply longer CP in order for the subframe to match exactly 0.5ms length. A proposed solution has 18 OFDM symbols with 71 samples long CP and 11 OFDM symbols with 70 samples long CP per subframe.

To conclude the issue, we summarize all the proposed settings in Table 4.3. We have to note that this numerology present fundamental changes to LTE. The philosophy stays the same, but whether components currently being developed for LTE could be reused, remains an open issue.

In our simulations, we use a combination of LTE's settings and the new proposal. Frequency domain settings are taken from the optimized structure, with one difference - one resource block is 12 subcarriers wide. This parameter was kept from release 8 in order to maintain the reference signal structure. The number of resource blocks was changed to 120, leading to full system bandwidth value of 86.4MHz. In time domain, we keep the LTE's layout completely, six OFDM symbols per time slot, with one pilot sequence in the middle. Such a time resource is about four times shorter than the local area proposal, however, it does not have much significance with low mobile station mobility.

Sample period	8.14ns
FFT size	2048
Subcarrier spacing	60kHz
CP in samples	49/70/71
Symbols in subframe	29
Subframe length	0.5ms
Subframes in frame	10
Frame length	5ms
Frame length in samples	614400
RB width [subcarriers]	10
RB width [frequency]	600kHz
RBs in 100MHz	150
CP overhead worst case	3.47%

Table 4.3 *Summary of proposed local area optimized numerology*

4.2.3 Channel modelling

In order to produce as trustworthy results as possible, we needed to find a reliable approach for channel modeling. Our focus is on system deployment in local areas, with high bandwidth and low mobility. Typical examples of such environment are office buildings and shopping malls and a radio channel in this conditions has its specific properties. These areas usually include many surrounding walls, therefore we would expect the transmitted signal to arrive from many directions. On the other hand, distances between handheld devices and base stations would be smaller than in outdoor cell, resulting in much shorter delay spread.

Choosing a proper model did not turn out to be a difficult task. 3GPP and 3GPP2 developed so called Spatial Channel Model SCM, however, that supports bandwidths only to 5MHz and offers only limited number of scenarios. Then we found out there is another multi-institutional project focusing on future wireless networks. It is called Wireless-World-Initiative-New-Radio (WINNER), and one of its working groups was pursuing research for new channel model. The research was split into two phases and went on for several years. The final outcome can be found in [18]. Matlab implementation [19] and also all other deliverables are available on WINNER webpages.

The first phase of the project, WINNER I, used 3GPP/3GPP2 SCM and IEEE 802.11n models as a starting point, former for outdoor and latter for indoor environments. However, in order to fulfill the requirements, original approaches had to be abandoned and new measurement-based models were developed. The new algorithm is geometry-based, with statistical distributions and channel parameters extracted from real-life measurements. WINNER I covered 2GHz and 5GHz deployment of these scenarios: indoor, typical urban micro-cell, typical urban macro-cell, sub-urban macro-cell, rural macro-cell and stationary feeder link.

WINNER II, the second phase, extended the model features, frequency range (2GHz to 6GHz) and the number of scenarios. The models from WINNER I were updated, and new degrees of freedom were added. The new scenarios cover indoor-to-outdoor, outdoor-to-indoor, bad urban micro-cell, bad urban macro-cell and others. Probably the most interesting addition is high

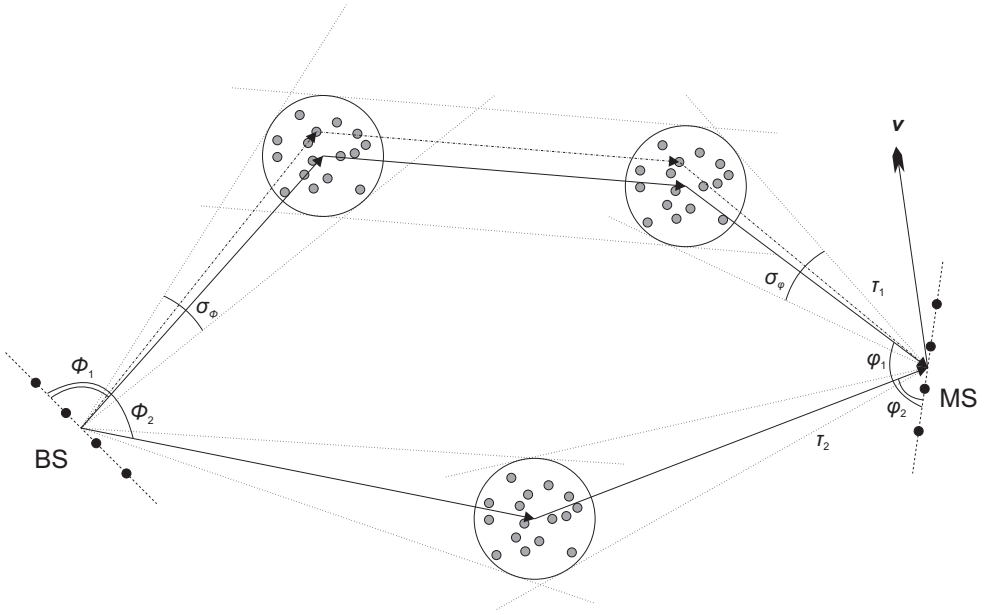

Figure 4.3 *WINNER single link model*

flexibility in defining antenna configurations, which can be very relevant in case of MIMO studies.

For our purposes, WINNER's indoor channel, called A1, was chosen. In the next two parts of the section we will describe WINNER II general modeling approach and details of deployment into our simulator.

Modeling approach

WINNER channel model is a geometry based stochastic model. A very good feature is separation of channel propagation properties and antenna configuration. Channel parameters are chosen stochastically, based on results from real-life measurements stored in memory. On the other hand, antenna geometries and parameters can be properly defined by user of the model.

With channel and antenna configurations set, the channel modeling itself is based on geometrical principle. Channel realizations are generated by summing contributions of planar waves, where each wave carries its specific small scale parameters like delay, power, angle of departure (AoD) and angle of arrival (AoA). Simulating larger number of waves leads to high precision of the model. With this approach, side effects like antenna correlation or Doppler effect are naturally embedded in the model.

We demonstrate WINNER single link model by Figure 4.3. We can see uniform linear arrays (ULA) of antennas at both base station and mobile station. Base station is static, while mobile station has a speed vector **v** assigned. Antenna parameters are not shown on the figure. Transmitted waves are reflected from blocks of scatterers, represented by circles filled with dots. This leads to increasing number of present waveforms (as shown on upper path), which are then summed in the receiver. What we can not see on the diagram is that there is such a channel for each transmit-receive antenna pair.

Transfer matrix of such MIMO link is

$$\mathbf{H}(t;\tau) = \sum_{n=1}^{N} \mathbf{H}_n(t;\tau), \tag{4.6}$$

where $\mathbf{H}_n(t;\tau)$ is a response matrix of one cluster n and N is the number of waves. Cluster is equal to propagation path diffused in space, either or both in delay and angle domains. It is a set of waveforms formed by reflection from block of scatterers. A cluster transfer matrix is given by

$$\mathbf{H}_n(t;\tau) = \iint \mathbf{F}_{rx}(\varphi)\mathbf{h}_n(t;\tau,\varphi,\phi)\mathbf{F}_{tx}^T(\phi)d\phi d\varphi, \tag{4.7}$$

where $\mathbf{F}_{tx}$ and $\mathbf{F}_{rx}$ are antenna array response matrices for transmitter and receiver, respectively, and $\mathbf{h}_n$ is a propagation channel response matrix for cluster n. Going even more into details, we can model a channel from transmitter antenna element s to receiver antenna element u for cluster n by

$$\begin{aligned} \mathbf{H}_{u,s,n}(t;\tau) = \ & \textstyle\sum_{m=1}^{M} \ \begin{bmatrix} F_{rx,u,V}(\varphi_{n,m}) \\ F_{rx,u,H}(\varphi_{n,m}) \end{bmatrix}^T \begin{bmatrix} \alpha_{n,m,VV} & \alpha_{n,m,VH} \\ \alpha_{n,m,HV} & \alpha_{n,m,HH} \end{bmatrix} \begin{bmatrix} F_{tx,s,V}(\phi_{n,m}) \\ F_{tx,s,H}(\phi_{n,m}) \end{bmatrix} \\ & \cdot \quad e^{j2\pi\lambda_0^{-1}(\bar{\varphi}_{n,m}\cdot\bar{r}_{rx,u})} e^{j2\pi\lambda_0^{-1}(\bar{\phi}_{n,m}\cdot\bar{r}_{tx,s})} \\ & \cdot \quad e^{j2\pi v_{n,m}t}\delta(\tau-\tau_{n,m}), \end{aligned} \tag{4.8}$$

where $F_{rx,u,V}$ and $F_{rx,u,H}$ are antenna element u field patterns for vertical and horizontal polarisations, respectively, $\alpha_{n,m,VV}$ and $\alpha_{n,m,VH}$ are complex gains of vertical-to-vertical and horizontal-to-vertical polarisations of wave n,m, respectively, λ_0 is wavelength of carrier frequency, $\bar{\phi}_{n,m}$ is AoD unit vector, $\bar{\varphi}_{n,m}$ is AoA unit vector, $\bar{r}_{tx,s}$ and $\bar{r}_{rx,u}$ are location vectors of antenna elements s and u, respectively, and $v_{n,m}$ is a Doppler frequency component of ray n,m. Furthermore, if we want a dynamic model with time evolution, all the above mentioned parameters are functions of time t.

Some of the link parameters can be seen in Figure 4.3. We refer the interested reader to WINNER deliverables. This model is also capable of simulating a large scale network with multiple links of different types. However, this feature is not needed for our work.

Implementation and context fitting

The research community behind WINNER II channel model has implemented it in Matlab and made it publicly available on WINNER webpages. The implementation is described in [19]. We did not used the final version of the code, where also antenna configuration in three dimensions was made possible. Instead, a second newest version, which is a bit simpler and thus more convenient, was used.

The code itself is quite straightforward to use. In the beginning, we set up a few parameters:

- Scenario is set to A1, WINNER II indoor model.
- Center frequency is set to 4GHz, which is an expected band for 100MHz local area deployment.

- Minimal, typical and maximal distance between base station and mobile station is set to 3m, 50m and 100m, respectively.
- Base station and mobile station heights are set to 1.5m.
- Velocity of mobile station movement is set to 3km/h, unless otherwise stated.

A choice of either line-of-sight (LOS) or non-line-of-sight (NLOS) model will be made dynamically, we will always comment on which one is used. On antenna configuration - we will use the default ULA structure. It is not a pattern typical for handheld device, however, it is simple and covers MIMO channel correlation in a sufficient way.

With the parameters set, the model produces either independent or time correlated realizations of the channel. The time evolution is simplified, as the tap positions remain the same from one snapshot to another. The taps do not disappear, nor do new taps emerge in the channel response. While this approach does not really follow reality, it is well justifiable in low mobility scenarios. And that is important for our work. As we model the channel by a tap-delay-line (TDL) model, the algorithm returns both tap values and tap positions in delay domain. To fit the output into our settings, we had to cover two additional issues:

- By default, the WINNER code constructs model of downlink channel. However, this is not difficult to overcome. By interchanging number of transmit and receive antennas and transposing channel response matrix, we apply principle of reciprocity and get the needed uplink version.
- The model returns tap delay values in 5ns steps. To fit it into our system, we need to change the sampling rate. A logical way would be to use a filter, but even the authors do not recommend it, because it would lead to creation of new taps. Instead, the original samples are moved to the nearest location in down-sampled grid. If multiple samples fall into the same tap, they are summed together.

4.3 Local area deployment

One of the crucial parts of this work is presented in this section. We take the described channel generation algorithm and use it for creation of wideband local area environment model. In such a scenario, we simulate link level performance of a system with given frame structure, using different MIMO approaches described in previous chapter. Separate sections are dedicated for enhancing the reception of single-layer transmission system and improving the spectral efficiency by means of dual-layer transmission.

4.3.1 Channel characteristics

Expected properties of local area wireless channel were already mentioned several times throughout previous sections. To summarize the comparison with typical urban cellular channels in a few words, we list the three most significant points:

- Delay spread is shorter, which leads to lower number of taps and decreased frequency selectivity.

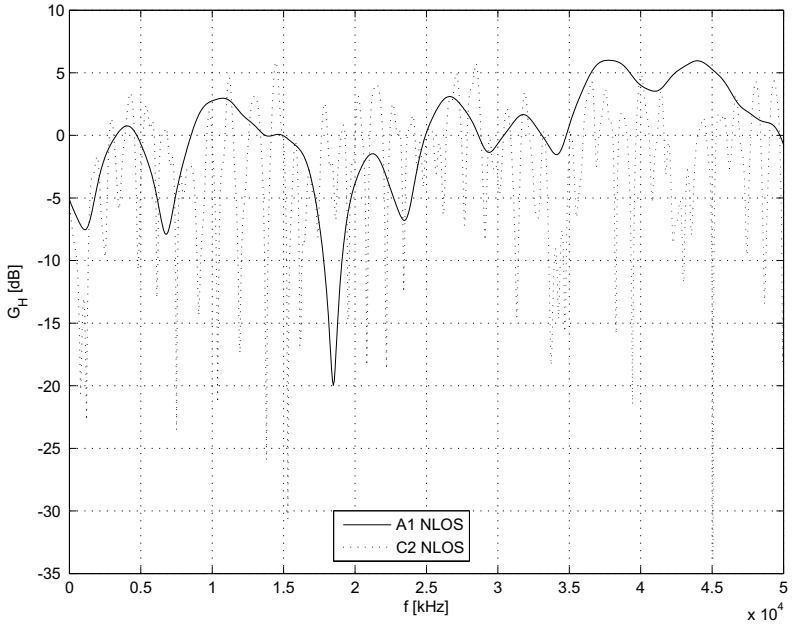

Figure 4.4 *Typical frequency profiles of local area and urban macro channels*

- Mobile terminals are static or slowly moving, therefore channel coefficients vary slowly in time.
- The spatial correlation is expected to be higher.

As an example of such environment, one can imagine deployment in office building, typically with small rooms and narrow corridors, shopping malls with different sized rooms and larger areas in between or maybe, in future, placement of low power base stations in our homes.

In section 4.2.3 we introduced state-of-the-art tool, which is able model a wide array of wireless scenarios. As we are interested in local areas, we choose the very first of them - indoor office, also called A1. In this section, we will use the WINNER II model to demonstrate some of the before-mentioned properties. In order to maintain compatibility with later link simulations, parameters from section 4.2.2, specifically FFT size 2048 and subcarrier spacing 60kHz.

Frequency profile

Starting with the first mentioned property, Figure 4.4 compares typical frequency domain shape of WINNER's A1 and C2 non-line-of-sight (NLOS) channels. A1 is an indoor office scenario, while C2 is an urban macro-cell scenario. The profiles are random realizations shown for the sake of example. No averaging or anything similar is used here.

To provide a more rigorous demonstration of low frequency selectivity, we present also plots of frequency domain correlation function. These were obtained by simulating 10^6 i.i.d. realizations of WINNER II model. The results are shown in Figure 4.5. This time we have also included A1 line-of-sight (LOS) scenario. Differences between the functions are significant, with C2 NLOS

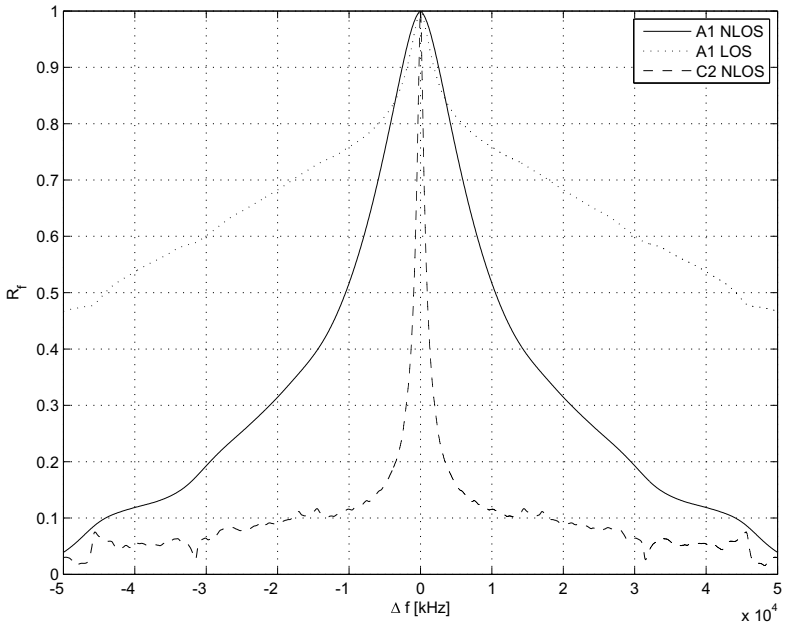

Figure 4.5 *Frequency domain correlation funtions of local area and urban macro channels*

being the most frequency selective channel, A1 NLOS being the second and A1 LOS the third. In order to quantify the results, we measured -3dB coherence bandwidths of the scenarios. The values are 540kHz, 5.82MHz and 17.1MHz for C2, A1 NLOS and A1 LOS, respectively.

Increased coherence bandwidth can have different impacts on system performance. It certainly is not good if there is no selectivity, which we could see in CDD introduction in section 3.1. This could happen for example if the scheduler assigns only a small part of the system bandwidth to certain user. In that case, different type of diversity should be introduced. On the other hand, higher frequency correlation can be beneficial from precoding granularity point of view. If the channel is similar in more resource blocks, it is likely that they would choose the same best precoding matrix. Controlling overhead could be reduced in this way.

Spatial correlation

Smaller spaces in indoor environments lead to increased spatial correlation. Again, we used our WINNER II model to demonstrate this phenomenon. The implementation allows us to set distance between multiple antennas on mobile station and base station, in fractions of wavelengths. There is also a possibility of specifying polarization and 3D placement parameters. However, for the sake of simplicity, we used the default ULA settings. The results for two transmit antennas in A1 NLOS and A1 LOS scenarios are shown in Figure 4.6.

The first very obvious result is that the presence of line-of-sight component increases the antenna correlation significantly. The simulations were made on mobile station antenna distance values from 0.01λ to λ, which makes a range of 0.75mm to 7.5cm on 4GHz center frequency. In a small handheld device the actual distance can be expected to be in this range. This means that

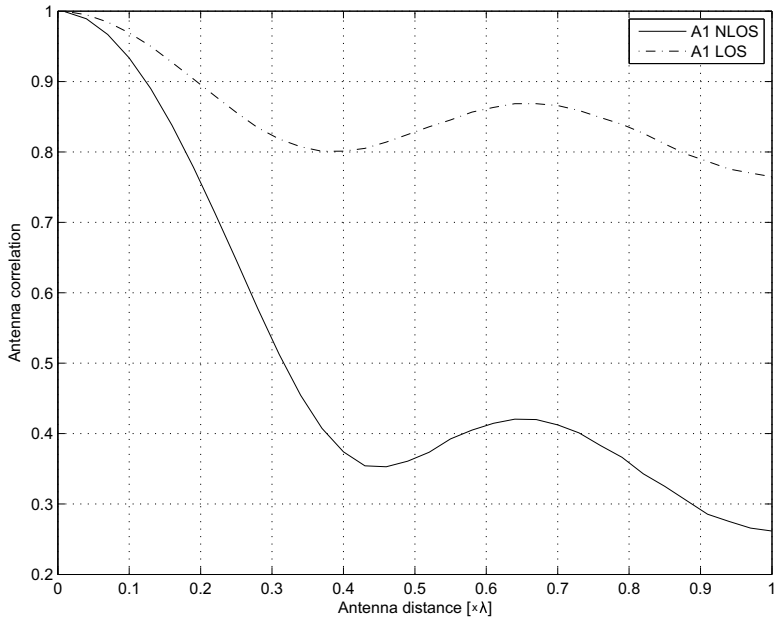

Figure 4.6 *MIMO channel correlation from transmit antenna point of view*

the correlation can be quite high, especially in case of LOS channel.

Increased spatial correlation leads to decreased diversity and is thus undesired by spatial diversity schemes like STBC or SFBC. Increased spatial correlation is also bad for spatial multiplexing. In case of two transmit antennas, increasing antenna correlation decreases the smaller singular value of the channel matrix, thus worsening the performance of the second layer. But, there is also one bright side of this issue - closed-loop beam-forming with constant modulus codewords can benefit from increased spatial correlation. It is because the transmission settings get closer to classical beam-forming, where changing antenna phases steers our signal into preferred direction.

Low mobility

Low user equipment velocity is naturally not a property of the channel itself. However, we do expect people in indoor environments to move slowly. This assumption leads to low Doppler shift and high channel correlation in absolute time domain. The fact that channel does not change fastly from one transmission subframe to another can be pick up by channel estimator.

To demonstrate the given advantage, we once again make use of WINNER II channel model. Since we use block fading approach, we create time correlated channel realizations for several subframes and apply the channel estimation algorithm described in section 4.1. We then compute estimation mean square error to channel gain ratio and compare the output with results from estimation with no time smoothing. We use A1 NLOS scenario, which is expected to be less time correlated, with mobile station velocity set to 3km/h.

It has to be noted that it may not be always possible to use time smoothing. With dynamic

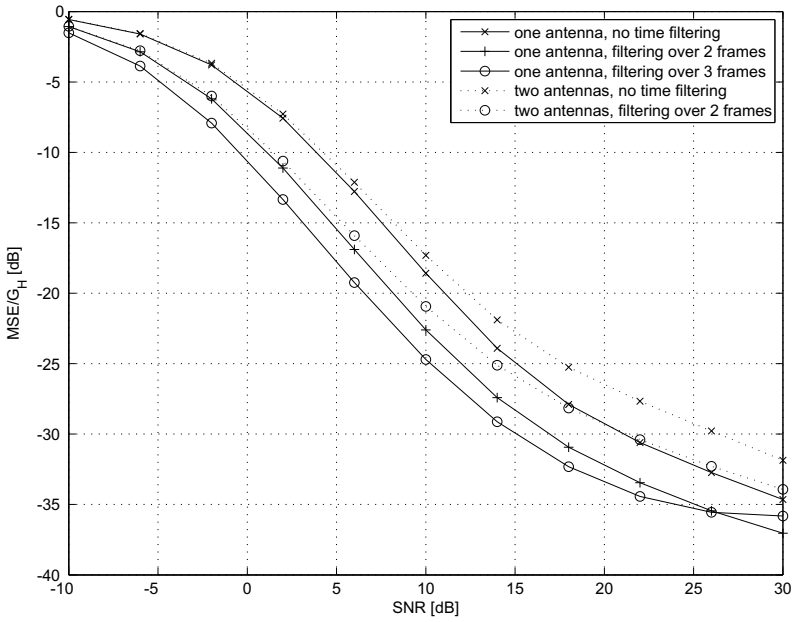

Figure 4.7 *Channel estimation performance improvement via time smoothing*

scheduling, subsequent time resources can be easily assigned to different users. Or, even if the same users gets a time slot again, it can be moved to different frequency in order to induce additional frequency selectivity. However, we bear in mind that proposed local area optimized frame is longer than the one we use. It may happen that more than one OFDM symbol will be replaced by pilot sequences, which would lead to a possibility of in-frame time smoothing.

The simulation results are shown in Figure 4.7. For both one and two transmit antennas, performance improvement by time smoothing is clearly visible. With one transmit antenna, we also present comparison of time smoothing through two and three subframes. The third subframe adds less gain, but it is still quite beneficial. In the highest SNR region, we can notice the effect of Doppler shift - the estimator performance does not improve anymore. With higher mobile station velocity, this effect would happen sooner (on lower SNR values).

4.3.2 Single-layer transmission

After extensive introductions and descriptions, in this section we finally start presenting link level simulation results. To keep in mind important modelling issues, we once again summarize the most important points. We created and used a single simulation platform, with features and details description listed in section 4.2.1. General simulator settings can be found in the beginning of section 4.2. We will use an indoor scenario of channel model developed by WINNER initiative, described in section 4.2.3. The frame structure we considered is defined in section 4.2.2.

We will start according to the same order as we described different MIMO algorithms in Chapter 3. Figure 4.8 presents throughput curves of CDD scheme in local area environment. The results are plotted for three different ECR values from [8] and compared to basic receive

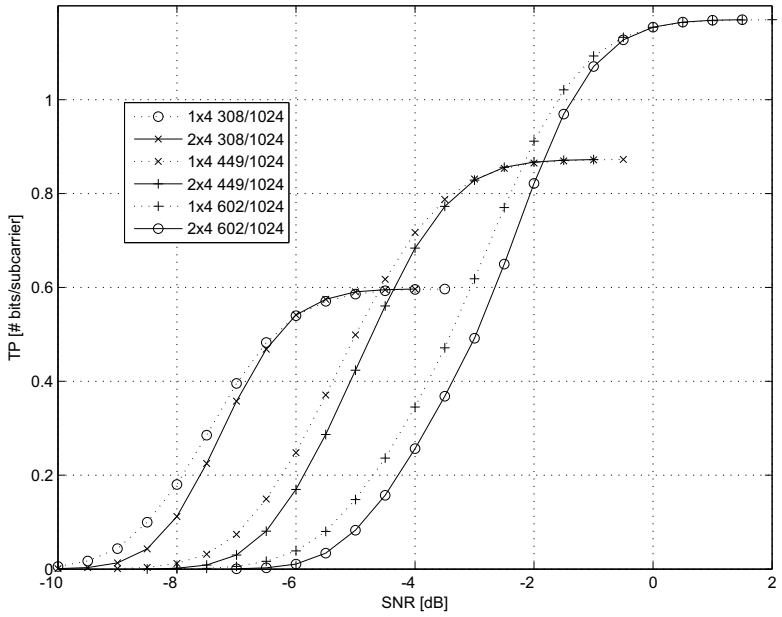

Figure 4.8 *Performance curves of CDD scheme in A1 NLOS channel*

diversity setting. The results are quite depressing - in the whole SNR range cyclic delay diversity actually worsens the performance. The reason is obvious - four receive antennas and wide user bandwidth (even with not-so-high frequency selectivity) provide enough diversity. Therefore, the parts of the spectrum that get better do not help the parts that get worse.

The situation changes when we deploy a scenario with smaller user bandwidth. On Figure 4.9, we compare different diversity schemes, but the user bandwidth is only four resource blocks (48 subcarriers) wide. Remembering Figure 4.5, this value is well below coherence bandwidth. The simulation ran with 308/1024 ECR and we can see that in higher SNR regions of this case, CDD can help. However, cyclic delay diversity still performs worse than SFBC, which despite higher computational requirements remains the preferred transmit diversity option.

Results for SFBC with three different ECR values are shown in Figure 4.10. In the important higher SNR regions, SFBC does not disappoint and brings reliable diversity improvement over one transmit antenna case. As stated in the general settings section, these simulation run with transmit antenna distance of 0.5λ, which according to Figure 4.6 means average transmit spatial correlation of 0.36. While defining SFBC, we already mentioned that it does not perform well in the presence of higher correlation. We present the comparison in higher SNR region in Figure 4.11.

Now moving on to beam-forming. We use codebook and subband settings from LTE. This means that subbands are 8 resource blocks (96 subcarriers) wide. We assume that the precoding matrix selector has an ideal channel knowledge and the feedback is instantaneous, with no errors in feedback messages. The immediate feedback can be justified well in low mobility scenarios. However, ideal CSI and error-free feedback can not. Our results can be found in Figure 4.12. As a codeword selection metric, we used Frobenius norm. The results are very promising. Comparing

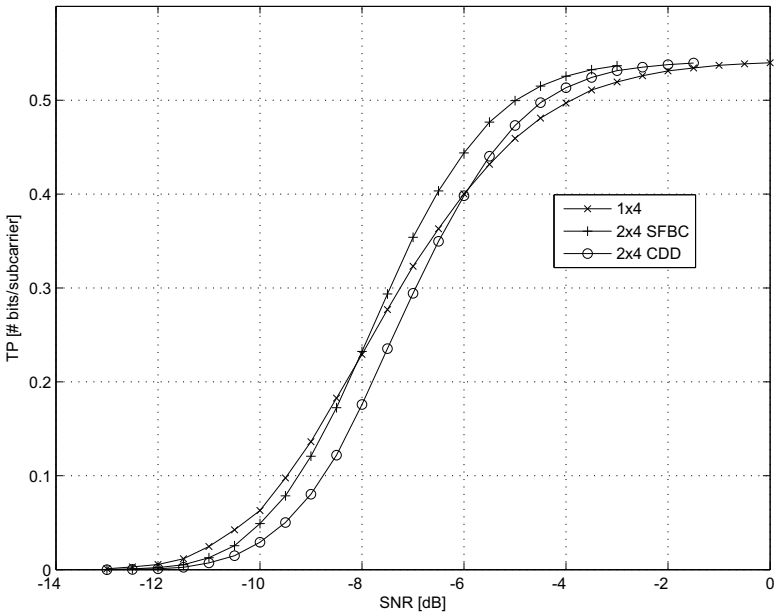

Figure 4.9 *Different diversity schemes in A1 NLOS scenario with small user bandwidth*

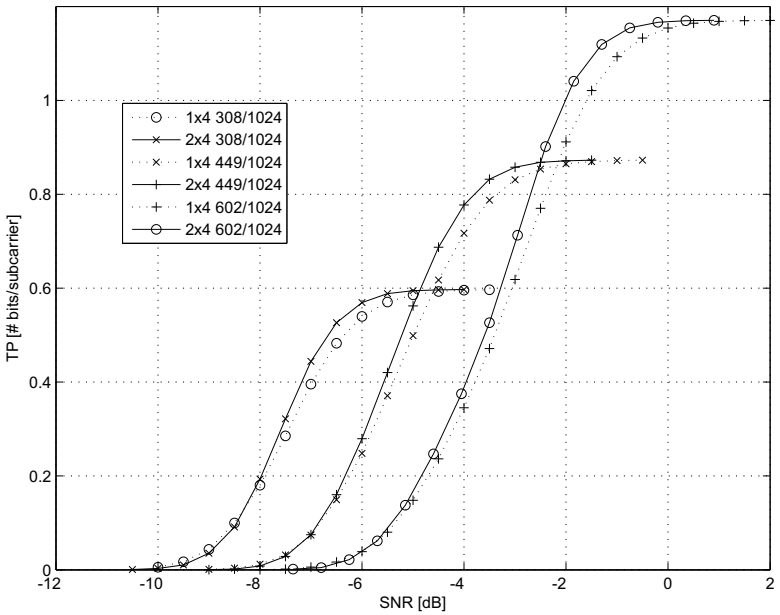

Figure 4.10 *Performance curves of SFBC diversity scheme in A1 NLOS channel*

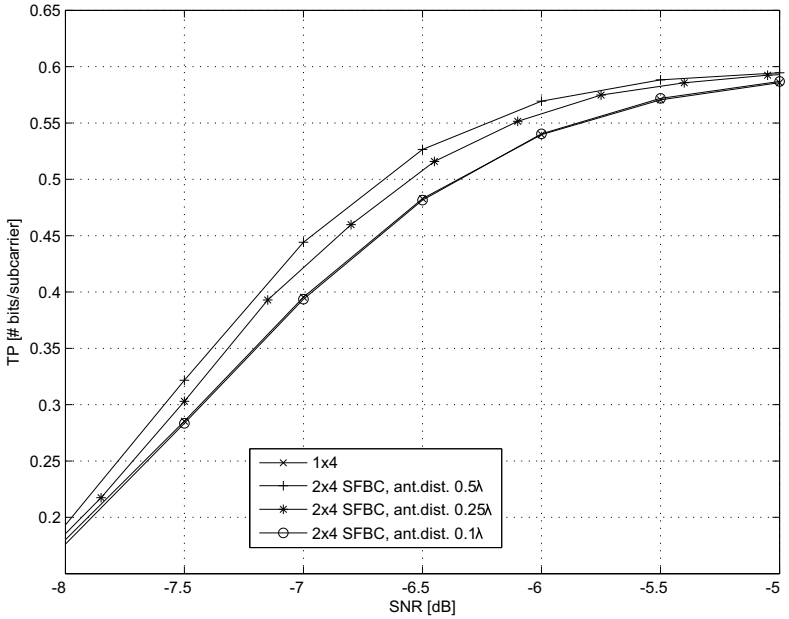

Figure 4.11 *Performance curves of SFBC with different antenna correlations*

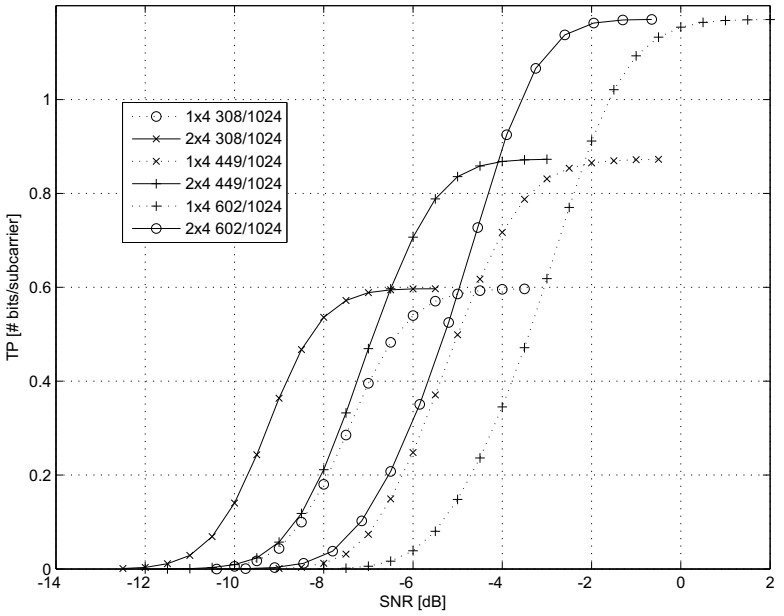

Figure 4.12 *Performance curves of codebook-based beam-forming in A1 NLOS channel*

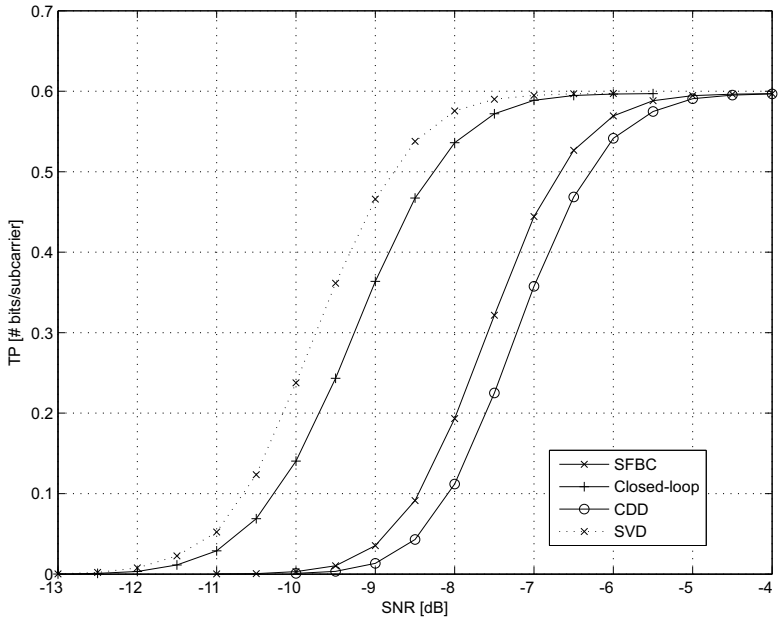

Figure 4.13 *Comparison of single-layer scheme performances*

to diversity schemes, beam-forming provides significant gain.

With all LTE's single-layer schemes simulated, we present one more plot. On Figure 4.13 we compare all of these schemes, running on 308/1024 ECR. Closed-loop is an obvious winner, with SFBC as an back-up option, if feedback controlling fails. No breakthrough here, the results agree with work that was done for LTE. On the plot there is also an SVD-based precoding curve, to see how far we are from optimality. There still is some gain to pursue and we will look into that in Section 4.4. We note here that all the simulations have been run in A1 NLOS scenario. We did so because NLOS is the weaker environment. An A1 LOS equivalent of Figure 4.13 is shown in Appendix A, Figure A.1. From the steeper slope of the curves we can observe that LOS is generally more favourable. However, CDD becomes completely useless and, thanks to increased spatial correlation, improvement by SFBC is also smaller.

4.3.3 Spatial multiplexing

The next step of improving the uplink capabilities should be a possibility to transmit multiple layers, just like in downlink. As we already noted, the final requirements for next 3GPP release are not set, but almost all the member companies want to include at least the option of having two transmit antennas with dual-layer transmission capability. This is also the scheme we chose to pursue. In this section, we will shortly present performance of LTE's dual-layer algorithms in wideband local area channel.

From the LTE point of view, we note here that especially the two antenna closed-loop standard does not receive much praise. The dual-layer codebook has only three codewords, while there is 16 of them in case of four transmit antennas. However, not much more can be done here - there

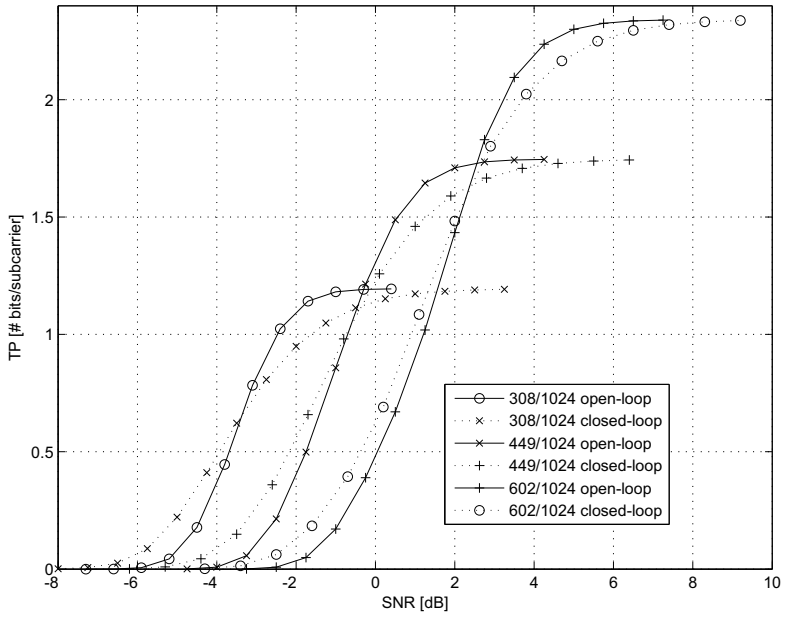

Figure 4.14 *LTE's open-loop and closed-loop dual-layer schemes in A1 NLOS channel*

are only two channel modes, and one of them is always weaker. The situation gets even worse in our case, where high transmit antenna correlation is expected. With higher correlation, the gain of the weaker mode is getting lower, because the channel matrix is closer to being linearly dependant.

In Figure 4.14, we present performance curves of LTE's open-loop and closed-loop dual-layer transmission schemes. We have included both in single plot, because there is no single-antenna option to compare them to. The simulations were run using our three typical MCS classes, in A1 NLOS scenario. The codeword selection metric for closed-loop scheme is MSV. Now, directly from the first glance we notice a very interesting discovery - in given scenario, the open-loop method with no feedback signalling actually performs better than the closed-loop option. It seems to go against the common sense, but the results speak for themselves. The combination of layer transformation and large delay CDD outperforms the three member codebook based design. We confirmed the same behavior also in A1 LOS scenario, but we will comment on that a bit later.

Following the same order from the previous section, we planned to compare the results with the optimal precoding scheme. However, immediately after seeing the first throughput curve, it became obvious that applying the typical LTE settings on dual-layer SVD-based precoding does not perform in the way we would typically expect. We are presenting one such scenario in Figure 4.15. We already know that by applying SVD, we decompose the MIMO channel into $\min(N_t, N_r)$ modes. These modes have different gains, and they are by default ordered in a descending manner. When we apply this on LTE's dual-layer settings with two Turbo coders, the first layer is always transmitted into the stronger mode and has better performance. The first three curves in Figure 4.15 are following this behaviour. The simulation was run with ECR value of 308/1024, in the A1 NLOS scenario. The first and second curve evaluate the perfomance of

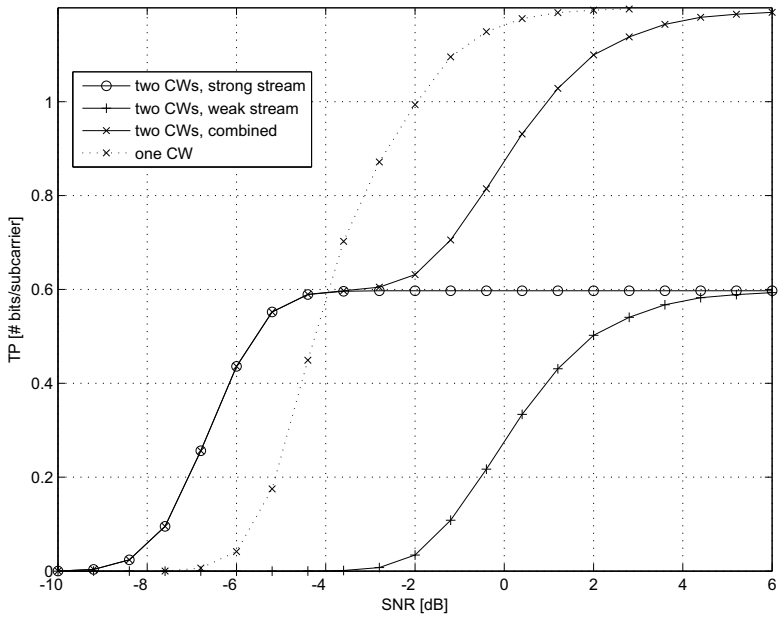

Figure 4.15 *Dual-layer optimal precoding curves with 308/1024 ECR*

the two transmitted layers separately, while the third one stands for overall system throughput.

Difference between throughputs of the two layers is significant. With this MCS class, the weaker layer starts to work only after the stronger one is already saturated. It may seem that the performance is good in the lower SNR region, but it is not the area where the setting is used. One possible way to solve a situation where one layer is working fine and the other is frequently asking for retransmissions, is to use a single Turbo codeword for both layers. We implemented the simplest possible alternative - every odd Turbo encoded bit is mapped into the first layer, and every even one into the second layer. In order to see the direct comparison, the performance curve of this option is also included in Figure 4.15. We can see that the errors from the weaker layer are spread across the single codeword, which resulted in somehow averaged performance. However, this can work only if ECR value is high enough. In Figure 4.16 we present the same situation with different MCS class, this time QPSK with 602/1024 ECR. In this case the Turbo code does not have enough parity bits to compensate for the erroneous layer.

As a last comparison of this section, we present Figure 4.17. It compares LTE's open-loop and closed-loop dual-layer scheme with SVD-based precoding with single Turbo codeword, all of them with 308/1024 ECR. In the relevant SNR area, open-loop spatial multiplexing beats even our pseudo-optimal scheme. This intensifies the fact that a different approach is needed for such environments. Optimal and quantized efforts of transmitting orthogonal layers does not give promising results.

Now we will come back to the mentioned A1 LOS confirmation. In Figure A.2, LTE's dual-layer open-loop and closed-loop schemes for three ECR values. Qualitatively, the comparison remains the same - closed-loop performs better in lower SNR region, and open-loop surpasses it in higher SNR region. But, because of significantly higher spatial correlation, spatial maltiplexing

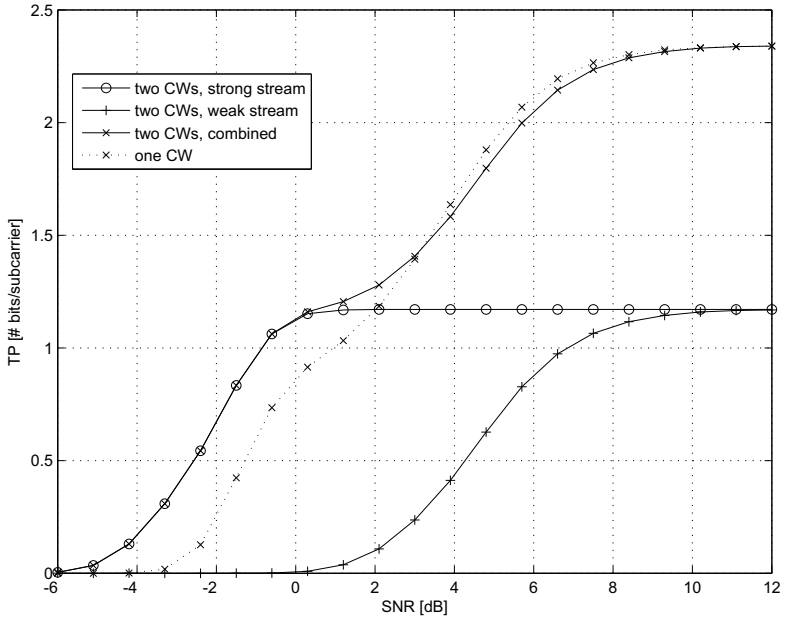

Figure 4.16 *Dual-layer optimal precoding curves with 602/1024 ECR*

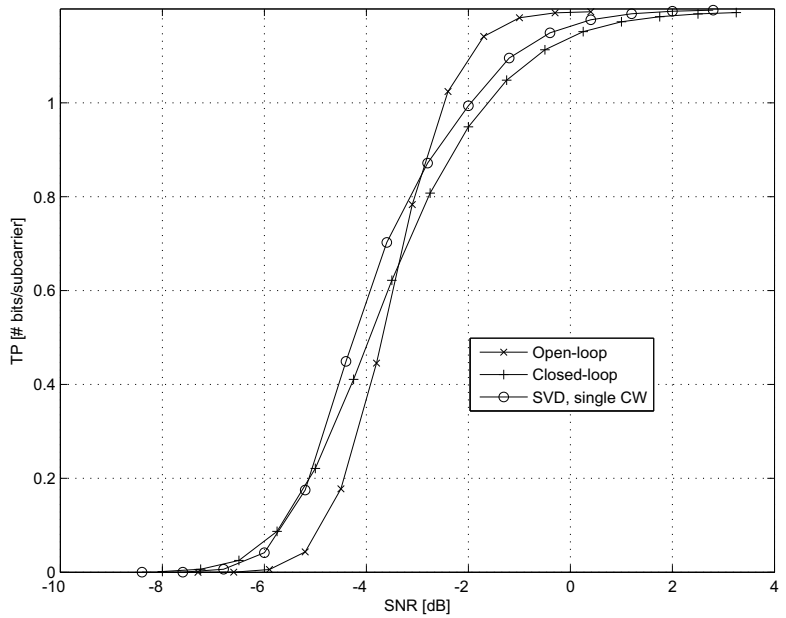

Figure 4.17 *Comparison of dual-layer transmission schemes*

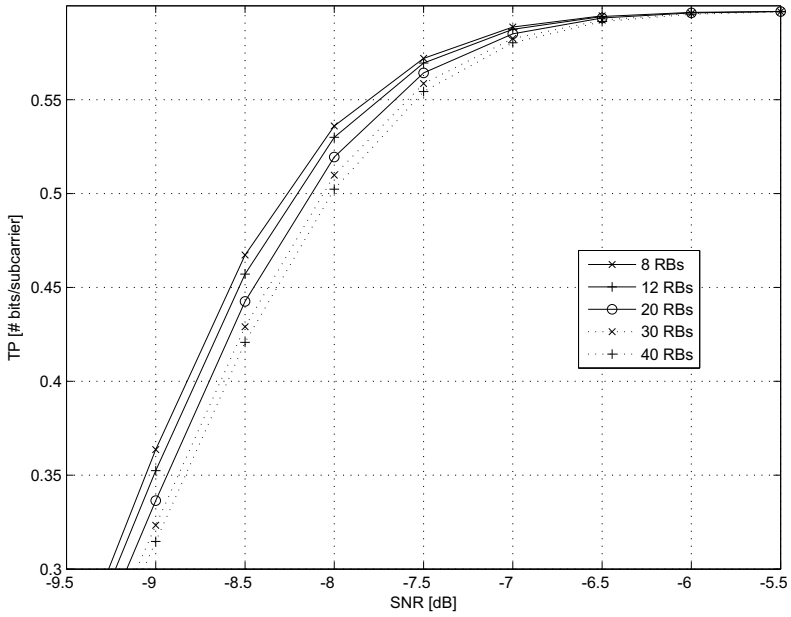

Figure 4.18 *Precoding subband granularity influence on single-layer transmission*

is getting more problematic. Especially the closed-loop performance starts to resemble optimal precoding. As a final observation, we state that the most probable reason behind open-loop's superior performance is the presence of layer transformation. Instead of sending each layer in separate channel mode, the transformation spreads both layers across the modes, resulting in somehow averaged throughput curve.

To conclude, we note here that there is one possible direction here that we did not pursue. And it actually seems very promising. When we realize that the channel modes have different gains, and that in case of single-layer transmission gain is the relevant parameter that influences the MCS choice, it would be logical to report different MCS class (CQI) per layer. The weaker layer can use higher ECR, or even fall for lower modulation order. This approach would require even more changes in the signalling message format, but if other problems with optimal precoding deployment are solved, it is the right way to go.

4.3.4 Subband granularity study

This section shortly demonstrates how precoding subband granularity influences the performance of closed-loop scheme in local area environment. We ran our simulations in A1 NLOS scenario, which has lower coherence bandwidth and therefore is more vulnerable to subband size changes. We use an ECR value of 308/1024, but the results are expected to be valid for general MCS class. The usual wideband transmission setting is modelled, and as a minimal subband size we use LTE's value for such a system, which is 8 resource blocks.

The performance curves are shown in Figures 4.18 and 4.19, for single-layer and dual-layer transmission separately. We plotted high SNR regions only, because those are the relevant parts

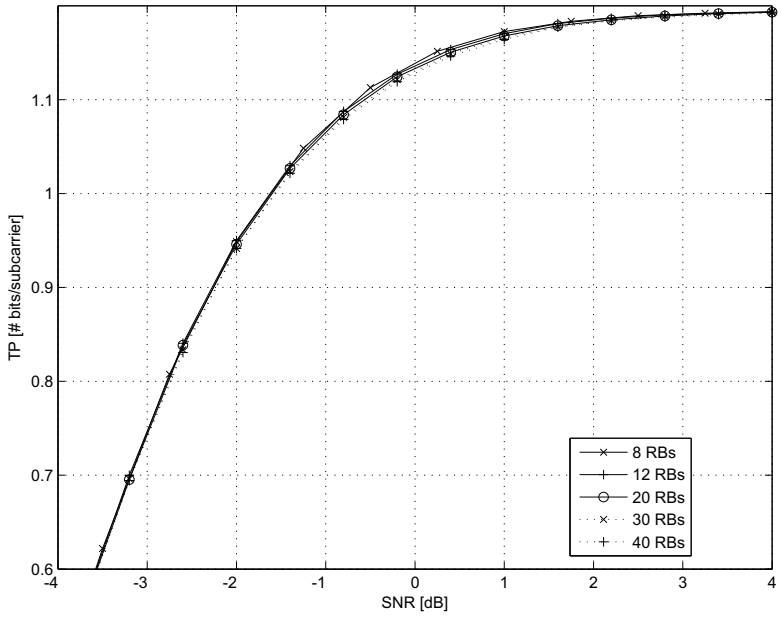

Figure 4.19 *Precoding subband granularity influence on dual-layer transmission*

and also because the differences can be seen better in such scale. Starting with the single-layer transmission - we expected a bit lower performance drop while increasing the size of the subband. However, with subcarrier spacing value of 60kHz, the simulated subband sizes are 5.76MHz, 8.64MHz, 14.4MHz, 21.6MHz and 28.8MHz wide. And keeping in mind frequency correlation function in Figure 4.5, these are already significant numbers. The situation gets very different for dual-layer transmission. There is very limited performance drop even in case of the highest simulated subband size. But, looking back at the performance of dual-layer closed-loop scheme, this case has to be further studied only if it is substantially improved.

Supported by our single-layer results, we recommend keeping LTE's subband granularity options.

4.4 Time division duplex system

Following the assignment of our work, we dedicate this section to ways of improving the performance from previous section in TDD system. Not to get confused, results from Section 4.3 are valid for both FDD and TDD deployments. However, TDD offers a possibility to efficiently implement SVD-based precoding. If we close our eyes for ceiling effect and spatial waterfilling, singular value decomposition provides the optimal precoding matrix. The scheme was introduced in Section 3.4. In Section 4.3.2 we used it for comparison with LTE's single layer transmission schemes, and in Section 4.3.3 we got even deep into it while simulating dual-layer performance in local area scenario. The algorithm requires full CSI at the transmitter. While in FDD this would lead to large feedback overhead, TDD offers a natural way of obtaining the CSI through channel

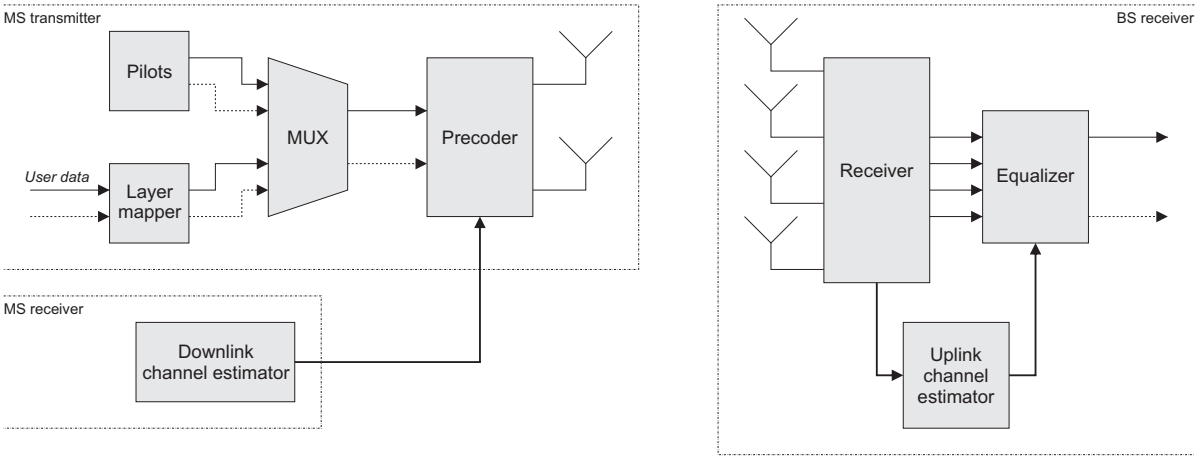

Figure 4.20 *Block diagram of reciprocity-based precoding scheme*

reciprocity.

While the practical settings for dual-layer optimal precoding are yet to be found, in case of single-layer transmission we were able to see some performance reserve of closed-loop scheme, when compared to SVD. In following parts of the section we will present a more detailed description of reciprocity-based optimal precoding system, identify and comment on its main weak points and at the end we will take a closer look at a problem that under a lot of discussion in standardization process - the necessity of UE calibration.

4.4.1 Reciprocity based MIMO approach

As a simple overview of SVD-based precoding taking advantage of channel reciprocity is depicted in Figure 4.20. We did not include time/frequency transformations and cyclic prefix additions in order to keep the diagram simple. The reader can compare the structure with a typical closed-loop layout available in Figure 3.8. Instead of feedback information, the output of downlink channel estimator is used to select optimal precoding matrix. This adds some mobile station complexity and requires a different approach for demodulation reference signals. As the receiver in base station does not know the precoding matrix, the whole $N_r \times \nu$ size equivalent channel matrix $\mathbf{H}_{eq}$ has to be estimated. This is achieved by applying precoding operation also on pilot symbols. It also means that there has to be one pilot sequence per transmission layer, instead of one sequence per transmit antenna in closed-loop case.

There are three big sources of possible performance degradation in our baseband model. They are listed here:

- Errors in downlink channel estimation procedure affect the precoder, resulting in sub-optimal precoding matrix choice. This phenomenon is also present in closed-loop, where PMI selection is based on uplink channel estimate. It cannot be helped.
- Precoding the demodulation reference signals complicates uplink channel estimation. A subband-based application of precoding matrix results in discontinuities in uplink equiv-

alent channel, which complicates smoothing in frequency domain. There is an ongoing research trying to solve this, but it remains out of our scope.

- Imperfections in mobile station's and base station's RF chain deform channel reciprocity. The precoder uses downlink channel estimate, which has downlink RF chain transfer functions embedded in itself. However, uplink RF transfer functions may be different. This issue we will pursue a bit deeper in Section 4.4.2.

4.4.2 RF chain imperfections

Transmit and receive RF chains distort the signal in every system, that is inevitable. It is the difference in these chains that cause problems in reciprocity based precoding. The mobile station estimates a channel, which has base station's transmit chain and mobile station's received chain transfer functions embedded. However, the optimal precoder needs information about uplink channel, which has mobile station's transmit chain and base station's receive chain transfer functions embedded. In this part of the section, we will model this mismatch and simulate its impact on link level performance.

In the frequency domain notation, we will model the RF chain transfer functions by diagonal matrices. The uplink channel is

$$\mathbf{H}_{ul} = \mathbf{R}_{BS}\mathbf{H}\mathbf{T}_{MS}, \tag{4.9}$$

where $\mathbf{H}$ is a $N_t \times N_r$ matrix of reciprocal channel, $\mathbf{R}_{BS}$ is a $N_r \times N_r$ transfer matrix of base station's receiver and $\mathbf{T}_{MS}$ is a $N_t \times N_t$ transfer matrix of mobile station's transmitter. In the same manner, the downlink channel will be

$$\mathbf{H}_{dl} = \mathbf{R}_{MS}\mathbf{H}^T\mathbf{T}_{BS}, \tag{4.10}$$

with $\mathbf{R}_{MS}$ and $\mathbf{T}_{BS}$ being $N_t \times N_t$ transfer matrix of mobile station's receiver and $N_r \times N_r$ transfer matrix of base station's transmitter, respectively. Now, we can write $\mathbf{H}_{ul}$ in terms of $\mathbf{H}_{dl}$ in following way:

$$\mathbf{H}_{ul} = \mathbf{R}_{BS}\mathbf{T}_{BS}^{-1}\mathbf{H}_{dl}^T\mathbf{R}_{MS}^{-1}\mathbf{T}_{MS} \tag{4.11}$$

Matrix $\mathbf{H}_{dl}$ is what we have from downlink channel estimator. Matrix $\mathbf{H}_{ul}$ is what we would like to have in order to calculate optimal precoding matrix. Everything else causes a uplink/downlink mismatch and possibly degrades performance of the precoder. To completely eliminate this problem, a complex calibration procedure would be required. Such an approach is not impossible, but it could mean increase in production costs of mobile terminals. And as one of the main 3GPP goals is to keep the price of user equipment as low as possible, the partnership companies are not eager to move in this direction.

We will not be solving here the calibration process itself, there is still an ongoing research covering it. However, we will demonstrate how the possible drop of performance could look like. The modelling will be based on calculation of optimal precoding matrix from deformed channel matrix and observing the impact on throughput curves. The deformed channel matrix $\mathbf{H}'$ will be

$$\mathbf{H}' = \mathbf{A}_{BS}\mathbf{P}_{BS}\mathbf{H}\mathbf{A}_{MS}\mathbf{P}_{MS} \tag{4.12}$$

Scenario number	σ^2_{Ba}	σ^2_{Bp}	σ^2_{Ma}	σ^2_{Mp}
1	0.5dB	$\frac{\arcsin(0.2)}{3}$	0.5dB	$\frac{\arcsin(0.2)}{3}$
2	1dB	$\frac{\arcsin(0.4)}{3}$	1dB	$\frac{\arcsin(0.4)}{3}$
3	1.5dB	$\frac{\arcsin(0.6)}{3}$	1.5dB	$\frac{\arcsin(0.6)}{3}$
4	2dB	$\frac{\arcsin(0.8)}{3}$	2dB	$\frac{\arcsin(0.8)}{3}$

Table 4.4 *Variance settings for mismatch simulations*

where **A** and **P** are square matrices modelling amplitude and phase mismatch, respectively. The mobile station mismatch matrices are given by

$$\mathbf{A}_{MS} = \begin{bmatrix} \sqrt{10^{\frac{N(0,\sigma^2_{Ma})}{10}}} & 0 \\ 0 & \sqrt{10^{\frac{N(0,\sigma^2_{Ma})}{10}}} \end{bmatrix}, \quad \mathbf{P}_{MS} = \begin{bmatrix} e^{jN(0,\sigma^2_{Mp})} & 0 \\ 0 & e^{jN(0,\sigma^2_{Mp})} \end{bmatrix}$$

where σ^2_{Ma} and σ^2_{Mp} are variances for amplitude and phase error in single antenna chain, respectively. For base station, the matrices would be 4×4 large. Here we show only the situation when all the errors are present at once. We simulate the typical 2x4 system, but this time we maintain optimality also in frequency domain - each subcarrier is precoded separately. The channel model is A1 NLOS and we use single-layer transmission with ECR value of 308/1024. The error variance values are shown in Table 4.4, and corresponding simulation results in Figure 4.21.

As we can see, the decrease of performance is significant. It is not known how high would the variances be in real scenario. We tried to base the range on *error vector magnitude* (EVM) defined in 3GPP specifications, however it is still more a guess than an estimate. Nevertheless, RF chain calibration has to be further studied, if reciprocity-based precoding is to be standardized.

The impact of separated errors is presented in Appendix A. From there we can conclude that mismatch in mobile station's RF chain cause much more trouble than those of base station's ($\mathbf{P}_{BS}$ has almost no degrading effect). It is good news, as this information would have to be signalled by means of control channel.

4.5 PAR analysis

In the last part of this chapter we shortly present one issue that has not been considered yet. All our local area simulations have been running with SC-FDMA. However, placement of MIMO algorithms into the frequency domain inevitably influences the praised 'single-carrier' property of this multiplexing scheme. On Figure 4.22 we show PAR probability curves of all single-layer transmission schemes. We observed PAR values of $2{\cdot}10^6$ simulated OFDM symbols, and then used the results to estimate probability of occurrence of these values. For comparison, we included curves of single-antenna settings with OFDMA and SC-FDMA. As we still observe baseband symbols, one would expect SC-FDMA to have a unit PAR value. That would happen if all FFT bins were used. Unused subcarriers at the band edges deteriorate it.

The results indicate that SC-FDMA still holds quite an advantage above OFDMA, even with MIMO steps applied in the frequency domain. CDD does not effect the PAR values at all. SFBC

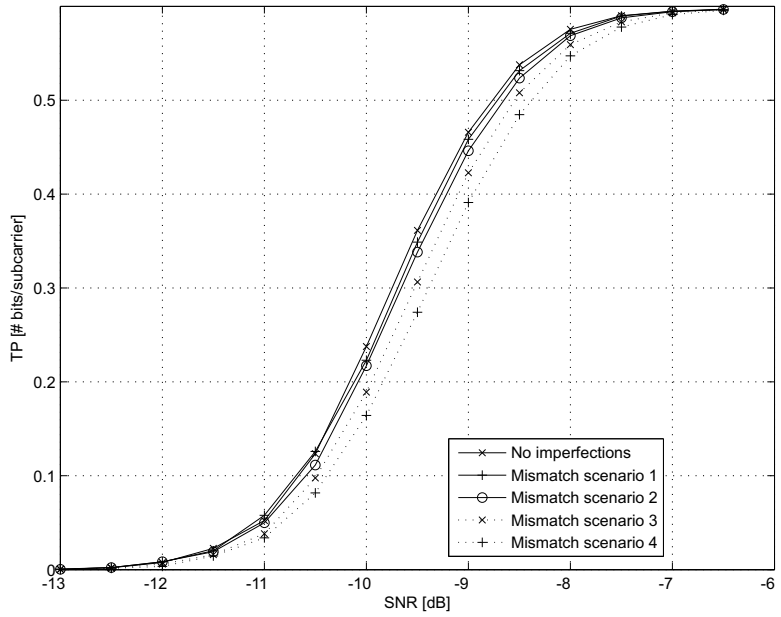

Figure 4.21 *Degradation of reciprocity through RF chain imperfections*

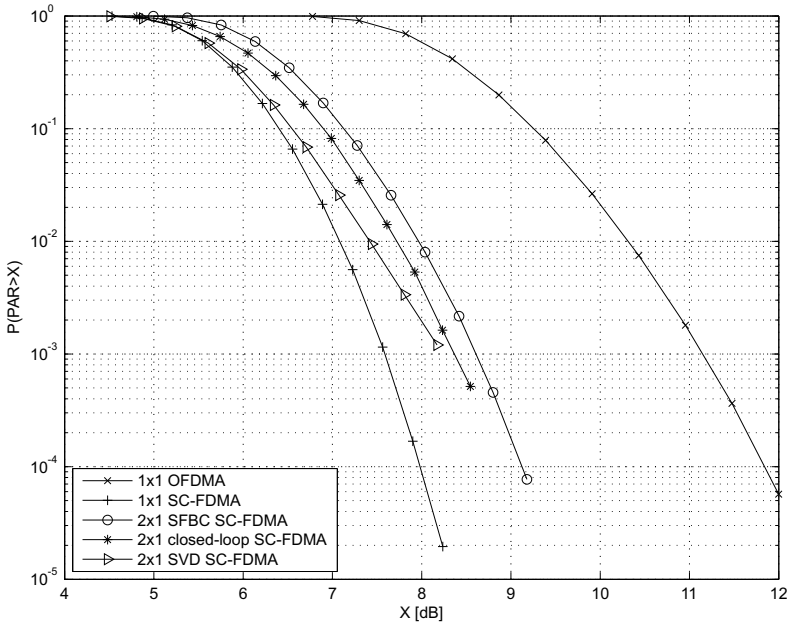

Figure 4.22 *PAR analysis of single-layer transmission schemes*

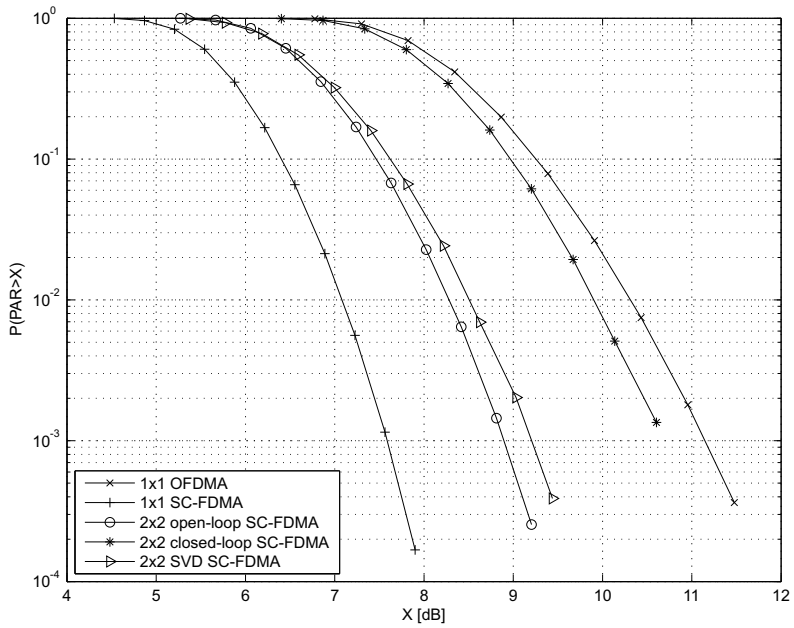

Figure 4.23 *PAR analysis of dual-layer transmission schemes*

and closed-loop beam-forming introduce slight deterioration on the second antenna. The PAR on the first antenna does not change, because the algorithms do not alter the symbols there. Optimal precoding affects both antennas, but the PAR increase is lower than in case of SFBC or closed-loop precoding. The highest deterioration is observed in case of SFBC diversity scheme.

The analysis for dual-layer transmission is shown on Figure 4.23. In this case, transmitted symbol on one resource element is influenced by both transmission layers, therefore we expect higher increase in PAR. The simulation results confirm this. All the schemes still sustain lower ratio than OFDMA case. However, dual-layer closed-loop precoding is very close. Open-loop spatial multiplexing and SVD-based precoding are approximately half-way between single-antenna SC-FDMA and OFDMA cases.

PAR values influence production costs of mobile stations. Some companies already proposed that in case of local area deployment, OFDMA should be used also for downlink. Our results indicate, that even in MIMO system, SC-FDMA can still produce more favourable shape of transmitted signal. The values increase, especially in case of spatial multiplexing, but the difference is still present.

Conclusion

Our thesis could be classified as a very basic step in introducing MIMO capabilities into uplink channel of LTE-A. The inclusion of multiple transmit antennas will inevitably lead to increased power consumption, therefore the study was focused on a scenario were high user throughputs are achievable - local area. Local area environments are typical for indoor areas. The system is expected to use TDD and wide frequency band. The 3GPP peak data rate target for uplink has been set to 500Mbps.

The descriptive part of the thesis started by introducing Long Term Evolution. We presented the basic architecture overview, with focus on the physical layer. Both uplink and downlink channels were mentioned. The chapter ended with the list of downlink MIMO algorithms, with a smooth transition into the next chapter where these schemes were described in more detailed manner. We also introduced the optimal precoding approach, as there is a possibility that it will find its way into TDD system.

The final chapter summarized the work that has been done through the months of our participation on the project. After short insight into possible system changes required by MIMO deployment we described the modelling platform that we prepared in order to get consistent and comparable simulation results. We dedicated one section to WINNER II channel model, which was used to provide realistic channel realizations. Then, the numerology choice for our simulations was chosen. We used most of the frequency domain parameters from proposed local area optimized frame structure, but kept the time domain options from LTE.

We started the local area simulations by analysis of local area channel. According to our expectations, the channel has lower frequency selectivity (in comparison with urban channels) and high antenna correlation. With line-of-sight component present, the channel has more favourable gain profile, but also much higher spatial correlation, than NLOS scenario. High spatial correlation can be picked up by closed-loop beam-forming with constant modulus codewords, but is not preferred by SFBC and spatial multiplexing in general.

The simulations of LTE's transmit diversity and beam-forming schemes with two transmit antennas lead to several conclusions. CDD can improve throughput only if there is not enough frequency selectivity (small part of the spectrum is assigned to user) and is always surpassed by SFBC. Codebook based closed-loop scheme remains the strongest player, providing very nice gains in all cases.

We continued by simulating the spatial multiplexing schemes. In general, two transmit antennas deployed with LTE settings in environment with possibility of high spatial correlation did not turn out to be a favourable scenario. In relevant high SNR regions, open-loop spatial multiplexing provided better performance than closed-loop one. According to further investigation, this was most probably caused by spreading the two layers through both channel modes. One

of the modes is always weaker, and separating the layers gives better results only in lower SNR regions.

The chapter ended with further insight into options in TDD and impact of MIMO on PAR values. In reciprocity-based mode, we concluded that the worst harm can be done if the mobile station is unaware of its RF receiver and transmitter chain transfer functions. As for PAR, it does increase. Not so much in single-layer transmission, but a lot more in case of spatial multiplexing. It has to be taken into account.

In the end, the MIMO design for uplink channel of the future system will most probably remain very conservative. We may see the deployment of optimal precoding based on SVD, but for that, the issues around estimation of the equivalent channel and RF chain calibration will have to be resolved. If not, codebook-based codeword selection with feedback reports will probably stay the principal multi-antenna scheme. The codebook itself may be redesigned, as there is still ongoing research in the field.

Bibliography

[1] "'3rd Generation Partnership Project; Technical Specification Group Radio Access Network; Requirements for Further Advancements for E-UTRA (LTE-Advanced) (Release 8)', 3GPP, 3GPP TR 36.913."

[2] A. Paulraj, R. Nabar, and D. Gore, *Introduction to Space-Time Wireless Communications*. Cambridge University Press, May 2003.

[3] "'3rd Generation Partnership Project; Technical Specification Group Radio Access Network; Requirements for Evolved UTRA (E-UTRA) and Evolved UTRAN (E-UTRAN) (Release 7)', 3GPP, 3GPP TR 25.913."

[4] E. Dahlman, S. Parkvall, J. Skold, and P. Beming, *3G Evolution: HSPA and LTE for Mobile Broadband*. Academic Press, 2007.

[5] D. F. et al, "Frequency Domain Equalization for Single-carrier Broadband Wireless Systems," *IEEE Communications Magazine*, vol. 40, pp. 58–66, April 2002.

[6] "'3rd Generation Partnership Project; Technical Specification Group Radio Access Network; Evolved Universal Terrestrial Radio Access (E-UTRA); Multiplexing and channel coding (Release 8)', 3GPP, 3GPP TS 36.212."

[7] "'3rd Generation Partnership Project; Technical Specification Group Radio Access Network; Evolved Universal Terrestrial Radio Access (E-UTRA); Physical Channels and Modulation (Release 8)', 3GPP, 3GPP TS 36.211."

[8] "'3rd Generation Partnership Project; Technical Specification Group Radio Access Network; Evolved Universal Terrestrial Radio Access (E-UTRA); Physical layer procedures (Release 8)', 3GPP, 3GPP TS 36.213."

[9] D. C. Chu, "Polyphase Codes with Good Periodic Correlation Properties," *IEEE Transactions on Information Theory*, vol. 18, pp. 531–532, July 1972.

[10] "'3rd Generation Partnership Project; Technical Specification Group Radio Access Network; Evolved Universal Terrestrial Radio Access (E-UTRA); Base Station (BS) radio transmission and reception (Release 8)', 3GPP, 3GPP TS 36.104."

[11] G. Bauch and J. S. Malik, "Orthogonal Frequency Division Multiple Access with Cyclic Delay Diversity," in *ITG Workshop on Smart Antennas*, pp. 17–24, IEEE, 2004.

[12] K. F. Lee and D. B. Williams, "A Space-Frequency Transmitter Diversity Technique for OFDM Systems," in *Global Telecommunications Conference*, pp. 1473–1477, IEEE, 2000.

[13] S. M. Alamouti, "A Simple Transmit Diversity Technique for Wireless Communications," *IEEE Journal on Selected Areas in Communications*, vol. 16, pp. 1451–1458, October 1998.

[14] A. Hottinen, O. Tirkkonen, and R. Wichman, *Multi-antenna Transceiver Techniques for 3G and Beyond*. John Wiley and sons, inc., January 2003.

[15] D. J. Love and R. W. Heath, "Limited Feedback Unitary Precoding for Spatial Multiplexing Systems," *IEEE Transactions on Information Theory*, vol. 51, pp. 2967–2976, August 2005.

[16] H. Meyr, M. Moeneclaey, and S. A. Fechtel, *Digital Communication Receivers*. John Wiley and sons, inc., October 1997.

[17] T. K. et al., "LTE-A Physical Layer Concept, Nokia/Nokia Siemens Networks internal report, 25.6.2008."

[18] "WINNER WP1: "WINNER II Channel Models", Deliverable D1.1.2 V1.1, 30.9.2007."

[19] L. Hentila, P. Kyosti, M. Kaske, M. Narandzic, and M. Alatossava, "MATLAB implementation of the WINNER Phase II Channel Model V1.1, December 2007."

Appendix A

Additional plots

A.1 Performance in A1 LOS scenario

We present here performance plots of LTE's single- and dual-layer schemes in A1 LOS scenarion. In comparison with A1 NLOS, A1 LOS MIMO channel has more favourable gain profile, is less frequency selective and more spatially correlated. The results of single-layer algorithms are shown in Figure A.1. According to those performance curves, CDD significantly deteriorates the throughput and SFBC provides smaller improvement than in LOS case. Closed-loop beamforming performs well, the improvement is a bit better. But that was expected, constant modulus codewords provide good results in highly correlated channels.

Dual-layer performance curves in Figure A.2 lead to same conclusion as in LOS channel, open-loop spatial multiplexing gives better throughput in higher SNR areas. The reason was mentioned before, the layer transformation spreads the layers across both channel modes. That does not happen with closed-loop precoding. As a result, one of the modes is significantly weaker (due to high spatial correlation), and the performance curves have step-like shape.

A.2 RF chain imperfections

As an addition to Section 4.4.2, impact of specific types of mismatches on reciprocity-based precoding is presented here. Figures A.3, A.4, A.5 and A.6 show performance drops caused by amplitude and phase errors in RF chains, both on base and mobile station's side. The values of phase error variances are identical to those in Table 4.4. It is clearly visible that the influences of $\mathbf{A}_{BS}$ and $\mathbf{P}_{BS}$ are smaller than those of $\mathbf{A}_{MS}$ and $\mathbf{P}_{MS}$. In fact, phase mismatch of base station's chain does not have almost any influence at all.

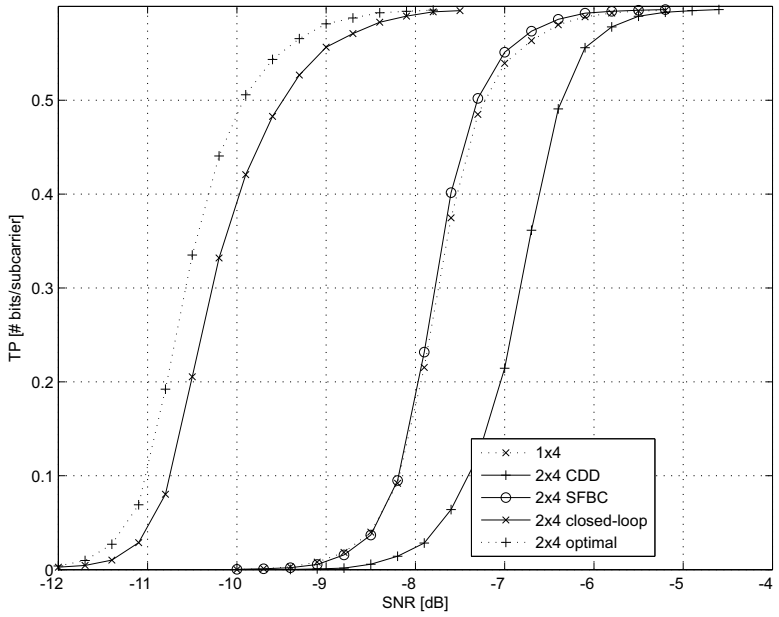

Figure A.1 *Performance of LTE's single-layer schemes in A1 LOS scenario*

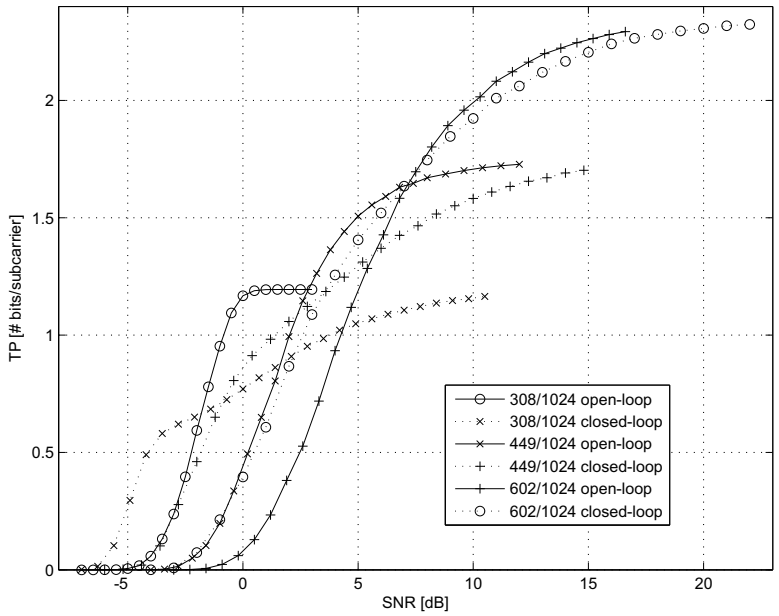

Figure A.2 *Performance of LTE's dual-layer schemes in A1 LOS scenario*

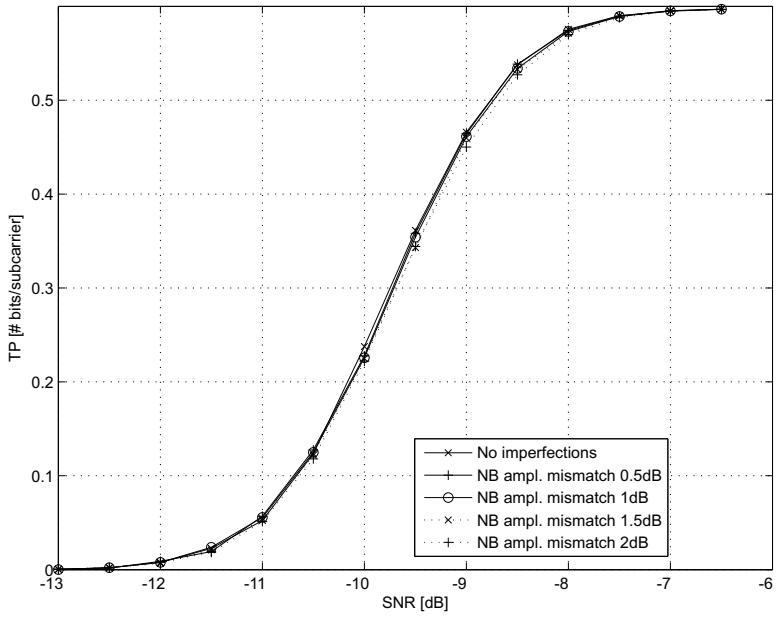

Figure A.3 *Optimal precoding performance degradation via* $\mathbf{A}_{BS}$

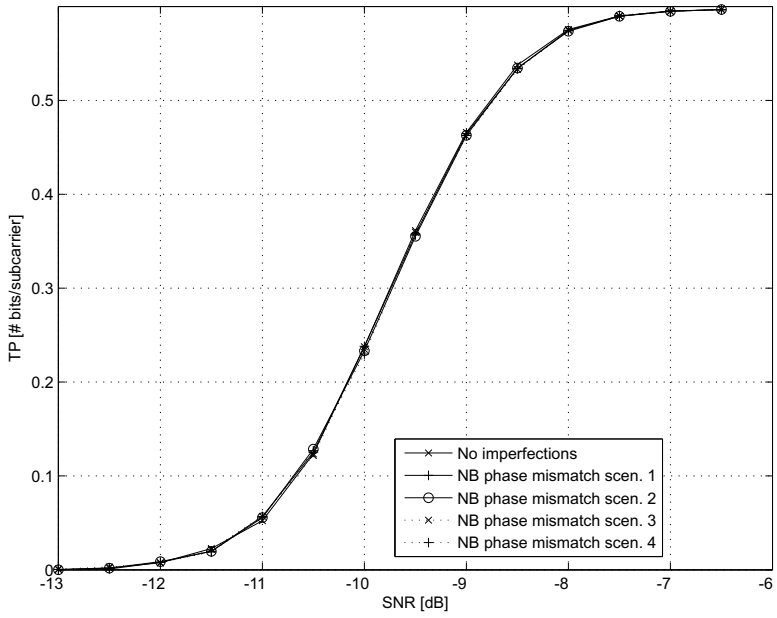

Figure A.4 *Optimal precoding performance degradation via* $\mathbf{P}_{BS}$

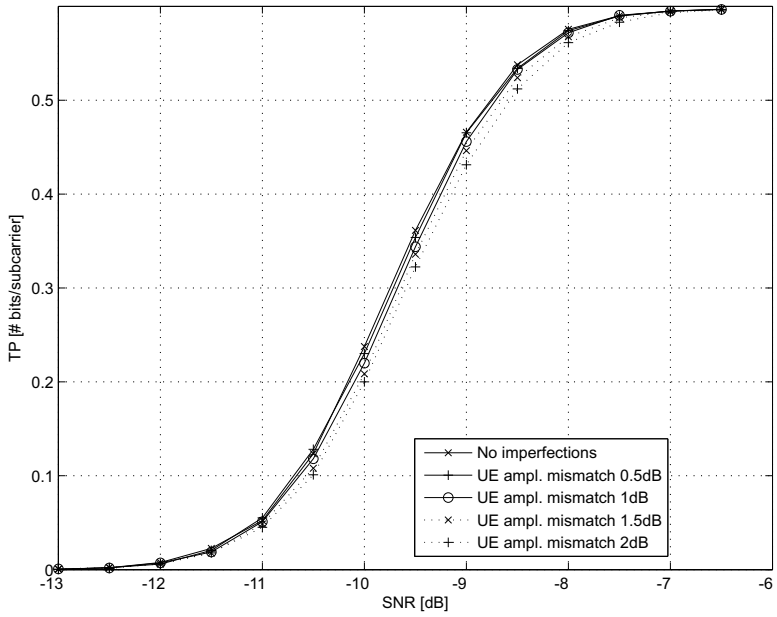

Figure A.5 *Optimal precoding performance degradation via* $\mathbf{A}_{MS}$

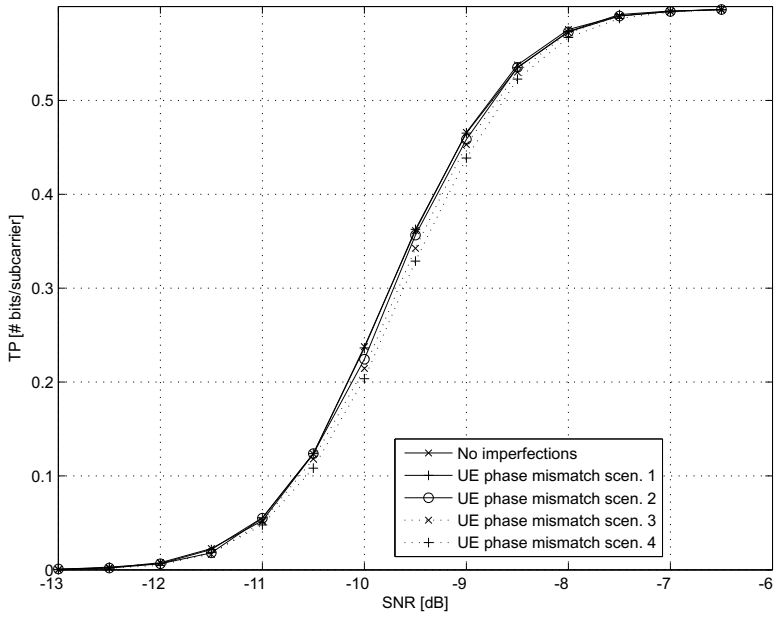

Figure A.6 *Optimal precoding performance degradation via* $\mathbf{P}_{MS}$